DEPARTMENT OF MATHEMATICS
COLLEGE OF SCIENCES
OLD DOMINION UNIVERSITY
NORFOLK, VIRGINIA 23529

COMPARISON OF LASER MODELS

By

John H. Heinbockel, Principal Investigator

Final Report
For the period ended May 15, 1992

Prepared for
National Aeronautics and Space Administration
Langley Research Center
Hampton, Virginia 23665

Under
Research Grant NAG-1-757
Dr. Robert C. Costen, Technical Monitor
Space Systems Division

May 1992

DEPARTMENT OF MATHEMATICS
COLLEGE OF SCIENCES
OLD DOMINION UNIVERSITY
NORFOLK, VIRGINIA 23529

COMPARISON OF LASER MODELS

By

John H. Heinbockel, Principal Investigator

Final Report
For the period ended May 15, 1992

Prepared for
National Aeronautics and Space Administration
Langley Research Center
Hampton, Virginia 23665

Under
Research Grant NAG-1-757
Dr. Robert C. Costen, Technical Monitor
Space Systems Division

Submitted by the
Old Dominion University Research Foundation
P.O. Box 6369
Norfolk, Virginia 23508-0369

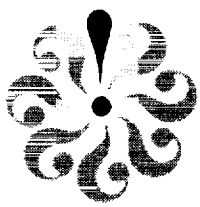

May 1992

FINAL REPORT NASA Grant NAG-1-757

The final phase of modeling solar pumped lasers considers the photodissociation of the perfloralkl molecules $n-C_3F_7I$,$t-C_4F_9I$ and $i-C_3F_7I$. Computer modeling has been compared to laboratory data and good agreement between theory and experiment has been achieved. The following is a summary of the modeling of solar pumped lasers.

A perfloride gas enters a tube at a point $z=0$ and travels a distance L at a velocity ω and then exits at the point $z=L$. During the flow the gas is solar pumped over the initial distance $0 \leq z \leq z_0$, where z_0 is less than or equal to L. The perfloride gas interacts chemically with light and a chain of chemical reactions occur.

CHEMICAL KINETICS

Following reference 1,2 and 3, let RI denote one of the perfluoralkl molecules, where R stands for either $n-C_3F_7$ or $t-C_4F_9$. The perfloralkl molecule flows through a circular tube where the gas is radially illuminated and pumped by the ultraviolet light in the 270 nm range and is characterized by the chemical reaction

$$RI+h\nu \xrightarrow{270\,nm} R+I^*,$$

where I^* is the $^2P_{1/2}$ excited state of iodine, which emits light at $1.315\mu\,m$. In addition, to the photodissociation reaction there are other chemical reactions which occur. These reactions are summarized as follows.

Photochemical Reactions for Iodine Laser Simulation

$$
\begin{aligned}
RI + h\nu_1 &\xrightarrow{\xi_1(0.27\,\mu m)} R + I^* \\
I_2 + h\nu_2 &\xrightarrow{\xi_2(0.5\,\mu m)} I^* + I \quad \text{(51 percent of the time.)} \\
I_2 + h\nu_2 &\xrightarrow{\xi_2(0.5\,\mu m)} I + I \quad \text{(49 percent of the time.)} \\
R_2 + h\nu_3 &\xrightarrow{\xi_3(1.32\,\mu m)} 2R \\
I^* + h\nu_4 &\xrightarrow{1.32\mu m} I + 2h\nu_4 \quad \text{Stimulated emission}
\end{aligned}
\tag{1}
$$

Regeneration reactions (rates have units $[cm^3/sec]$)

$$
\begin{aligned}
I^* + R &\xrightarrow{k_1} RI \\
I + R &\xrightarrow{k_2} RI \\
R + R &\xrightarrow{k_3} R_2 \\
R + RI &\xrightarrow{k_4} R_2 + I \\
R + I_2 &\xrightarrow{k_5} RI + I \\
R + RI &\xrightarrow{k_6} R_2 + I^* \\
I^* + RI &\xrightarrow{k_7} I_2 + R \\
I + RI &\xrightarrow{k_8} I_2 + R
\end{aligned}
\tag{2}
$$

Quenching reactions (rates have units $[cm^3/sec]$)

$$
\begin{aligned}
I^* + RI &\xrightarrow{q_1} I + RI \\
I^* + I_2 &\xrightarrow{q_2} I + I_2 \\
I^* + R &\xrightarrow{q_3} I + R \\
I^* + R_2 &\xrightarrow{q_4} I + R_2 \\
I^* + I &\xrightarrow{q_5} I + I
\end{aligned}
\tag{3}
$$

Three body collision reactions (rates have units $[cm^6/sec]$)

$$\begin{aligned} I^* + I + RI &\xrightarrow{c_1} I_2 + RI \\ I + I + RI &\xrightarrow{c_2} I_2 + RI \\ I^* + I + I2 &\xrightarrow{c_3} I_2 + I_2 \\ I + I + I_2 &\xrightarrow{c_4} I_2 + I_2 \\ I + I + R_2 &\xrightarrow{c_5} I_2 + R_2 \\ I + I^* + R_2 &\xrightarrow{c_6} I_2 + R_2 \end{aligned} \tag{4}$$

Wall reactions (rates have units $[cm^3/sec]$)

$$\begin{aligned} I + I + Wall &\xrightarrow{v_1} I_2 + Wall \\ I + R_2 + Wall &\xrightarrow{v_2} R + RI + Wall \end{aligned} \tag{5}$$

Pyrolysis reactions (rates have units $[cm^3/sec]$)

$$\begin{aligned} RI+ &\xrightarrow{k_9} R + I \\ R_2 &\xrightarrow{k_{10}} R + R \end{aligned} \tag{6}$$

In the above reactions note that we have denoted by
$q_i, i = 1, ...9$ those reaction rates which are quenching;
$k_i, i = 1, ..., 8$ those reaction rates which are regenerative;
$k_i, i = 9, 10$ those reaction rates which are due to pyrolysis;
$v_i, i = 1, 2$ the reaction rates of wall reactions;
$c_i, i = 1, 6$ those reaction rates due to three body collisions.

The dimension of the reaction rates are s^{-1} for single particle decomposition; $cm^3\, s^{-1}$ for binary collisions and $cm^6\, s^{-1}$ for three body collisions.

RATE COEFFICIENTS

The reaction rate coefficients are assigned the following values for $n - C_3F_7I$.

Regenerative and pyrolysis

$$k_1 = 1.0\,(10)^{-14} \qquad k_6 = 0.0$$

$$k_2 = 2.3\,(10)^{-11} \qquad k_7 = 3.0\,(10)^{-19}$$

$$k_3 = 6.5\,(10)^{-13} \qquad k_8 = 1.6\,(10)^{-23}$$

$$k_4 = 3.0\,(10)^{-16} \qquad k_9 = 1.0\,(10)^{15}\,\exp(-2.48((10)^4)/T)$$

$$k_5 = 5.0\,(10)^{-11} \qquad k_{10} = 1.0\,(10)^{17}\,\exp(-4.73((10)^4)/T)$$

Three body

$$c_1 = 1.6\,(10)^{-33}$$

$$c_2 = 5.7\,(10)^{-33}\exp(1360/T)$$

$$c_3 = 0.0$$

$$c_4 = (10)^{-29.437-5.844Log10(T/300)+2.163(Log10(T/300))^2}$$

$$c_5 = 8.0\,(10)^{-33}\,\exp(1310/T)$$

$$c_6 = 0.0$$

Quenching

$$q1 = 1.7\,(10)^{-17}$$

$$q2 = 2.9\,(10)^{-11}\,\exp(-4.4(10)^{-3}(T - 300))$$

$$q3 = 3.7\,(10)^{-18}$$

$$q4 = 4.7\,(10)^{-16}$$

$$q5 = 1.6\,(10)^{-14}$$

Pumping and Lasing

$$v1 = 0.0$$

$$v2 = 0.0$$

$$\xi_1 = 1.2\,(10)^{-2}\,(n - C_3F_7I)$$

$$\xi_2 = 0.12\,(n - C_3F_7I)$$

$$\xi_3 = 0.0$$

Note that many of the coefficients are temperature dependent, where T is the absolute temperature. In addition, certain reactions, although postulated, are not readily known. For example, the effect of wall reactions. These postulated reactions, though used in some of the preliminary studies, have been set to zero by setting the reaction rate coefficients to zero. The ξ_1 and ξ_2 coefficients are multiplied by the pump power density in solar constants and $\xi_3 = 0$ coefficient is associated with one of the postulated reactions which was removed. The above reaction kinetics are in basic agreement with those given in references 1,2,3,4 and 5.

DIFFERENTIAL EQUATIONS FOR REACTION KINETICS

Using the law of mass action, the above set of chemical kinetics are replaced by a coupled system of ordinary differential equations. We denote the concentration of the various chemical reactants by

$$x_1 = [RI], \quad x_2 = [R], \quad x_3 = [R_2], \quad x_4 = [I_2],$$
$$x_5 = [I^*], \quad x_6 = [I], \quad x_7 = \rho_+, \quad x_8 = \rho_-$$

where ρ_+ and ρ_- are photon densities to be discussed shortly. The chemical kinetics can now be represented in the form

$$\frac{dx_i}{dt} = \frac{\partial x_i}{\partial t} + \left(\vec{V} \cdot \nabla\right) x_i + x_i \nabla \cdot \vec{V} = f_i(\bar{x}), \quad i = 1, \ldots, 6$$

where, $\bar{x} = (x_1, x_2, x_3, x_4, x_5, x_6)$ and $\vec{V} = \omega\, \hat{e}_z$ is the flow velocity in the z direction. Here $(\vec{V} \cdot \nabla) x_i$ is a convective term and $x_i\, \nabla \cdot \vec{V}$ is a dilatation term. For steady state conditions we write the system in the form

$$\omega \frac{dx_i}{dz} = f_i(\bar{x}) - x_i \frac{d\omega}{dz} = F_i(\bar{x}), \quad i = 1, ..., 6.$$

where $f_i, i = 1, ..., 6$ represents the right hand side of the above system of equations and are given by

$$
\begin{aligned}
f_1(\bar{x}) =& k_1[R][I^*] + k_2[R][I] - k_7[I^*][RI] - k_4[R][RI] \\
& - k_6[R][RI] - \xi_1[RI] + v_2[R_2][I] + k_5[R][I_2] - k_9[RI] \\
f_2(\bar{x}) =& \xi_1 - k_1[R][I^*] - k_2[R][I] - 2k_3[R]^2 - k_4[RI][R] \\
& - k_6[RI][R] - k_5[R][I_2] + v_2[R_2][I] + k_7[RI][I^*] + k_8[I][RI] + k_9[RI] \\
& + 2k_{10}[R_2] - [R]/\tau_2 \\
f_3(\bar{x}) =& k_3[R]^2 + k_6[RI][R] + k_4[RI][R] - v_2[R_2][I] - k_10[R_2] - [R_2]/\tau_3 \\
f_4(\bar{x}) =& - \xi_2[I_2] + c_1[RI][I^*][I] + c_2[RI][I]^2 + c_3[I_2][I^*][I] + c_4[I_2][I]^2 \\
& + k_7[RI][I^*] - k_5[R][I_2] + v_1[I]^2 \\
& + c_5[I]^2[R_2] + k_8[RI][I] + c_6[I][I^*][R] - [I_2]/\tau_4 \\
f_5(\bar{x}) =& Q_y\xi_1[RI] + 0.51\xi_2[I_2] - k_1[R][I^*] - q_2[I_2][I^*] - c\sigma([\rho_+] + [\rho_-])([I^*] - \frac{1}{2}[I]) \\
& + k_6[R][RI] - q_3[R][I^*] - q_4[R_2][I^*] - q_5[I^*][I] - k_7[RI][I^*] \\
& - c_6[R_2][I^*][I] - c_1[RI][I^*][I] - c_3[I_2][I^*][I] - q_1[RI][I^*] - [I^*]/\tau_5 \\
f_6(\bar{x}) =& 1.49\xi_2[I_2] + q_1[RI][I^*] + q_2[I_2][I^*] - 2c_5[I]^2[R_2] - k_8[I][RI] \\
& c\sigma([\rho_+] + [\rho_-])([I^*] - \frac{1}{2}[I]) - c_1[RI][I^*][I] - 2c_2[RI][I]^2 - c_3[I_2][I^*][I] \\
& - 2c_4[I_2][I]^2 - k_2[R][I] + k_4[RI][R] + q_3[I^*][R] + q_4[I^*][R_2] \\
& + q_5[I^*][I] + k_5[R][I_2] - v_2[R_2][I] - 2v_1[I]^2 - c_6[R_2][I^*][I] + k_9[RI] - [I]/\tau_6 \\
f_7(\bar{x}) =& c\sigma[\rho_+]([I^*] - \frac{1}{2}[I])
\end{aligned}
\tag{7}
$$

where Q_y is the quantum yield and the terms involving τ_i, $i = 2, ..., 6$ represent diffusion effects. Without the diffusion terms, the above system of nonlinear differential equations conserves the masses of the species involved in the reactions and for steady state operation at any point z we have the immediate integrals

$$
\begin{aligned}
[RI] + [R] + 2[R_2] =& Constant \\
[RI] + 2[I_2] + [I^*] + [I] =& Constant.
\end{aligned}
\tag{8}
$$

provided the diffusion terms are removed.

The above coupled system of nonlinear ordinary differential equations are subject to the initial conditions that at $z = 0$ we have

$$
x_1 = B, \qquad x_i = 0.0 \quad \text{for} \quad i = 2, \ldots, 6,
$$

where $B = 9.66\,(10)^{18}\,P/T$ is the initial concentration of $[RI]$ which is dependent upon the inlet pressure P (torr) and absolute temperature T.

The above system of differential equations is scaled in both the dependent and independent variables. The steady state independent variable is z which varies between 0 and L. This distance is scaled to the interval $0 \leq s \leq 1$ by making the substitution $z = sL$. The dependent variables are scaled by the substitutions

$$x_i = By_i, \quad i = 1, \ldots 7,$$

and the initial conditions upon $y_i, i = 1, \ldots, 6$ become $y_1(0) = 1.0$ and $y_i(0) = 0.0$ for $i = 1, ..., 6$.

In addition to these chemical variables let ρ denote the photon density in the laser tube which has a length L. Assume $\rho = \rho_- + \rho_+$, where ρ_+ is the number of photons per cubic centimeter moving to the right and ρ_- is the number of photons moving to the left. From reference 1, the photon density satisfies the differential equation

$$\frac{d\rho_+}{dt} = c\sigma\rho_+ \left([I^*] - \frac{1}{2}[I]\right)$$
$$\frac{d\rho_-}{dt} = c\sigma\rho_- \left([I^*] - \frac{1}{2}[I]\right)$$

where c is the speed of light, σ is a capture cross section, $[I^*]$ is the concentration of excited state of iodine, and $[I]$ is the concentration of iodine.

Photon Density Equation

Let the light flux density of the lasing photon be denoted by $\rho = \rho_+ + \rho_-$ where $\rho_+ = \rho_+(z,t)$ denotes the photon density propagating in the positive z direction and $\rho_- = \rho_-(z,t)$ denotes the photon density propagating in the negative z direction. The differential equations for these photon densities are

$$\frac{1}{c}\frac{\partial\rho_+}{\partial t} + \frac{\partial\rho_+}{\partial z} = \sigma\rho_+([I^*] - \frac{1}{2}[I])$$
$$\frac{1}{c}\frac{\partial\rho_-}{\partial t} - \frac{\partial\rho_-}{\partial z} = \sigma\rho_-([I^*] - \frac{1}{2}[I])$$

where c is the speed of light in the optical medium, and σ is a capture cross section. In the above equations $\sigma[I^*]\rho_+$ is the amplification factor resulting from population of the upper

laser level of the active medium and $-\frac{1}{2}\sigma[I]\rho_+$ is the decrease in photon density due to population of the lower lasing level.

Note that for steady state conditions the quantities ρ_+ and ρ_- satisfy the differential relation

$$\rho_+ \frac{d\rho_-}{dz} + \rho_- \frac{d\rho_+}{dz} = 0 \tag{9}$$

and consequently by direct integration we find that

$$\rho_+(z)\rho_-(z) = K_0 = Constant. \tag{10}$$

Denote by R_1 and R_2 the reflectivities of the mirrors then we will have the boundary conditions

$$\rho_+(0) = R_1\rho_-(0) \qquad \text{and} \qquad \rho_-(L) = R_2\rho_+(L),$$

as illustrated in the figure 1.

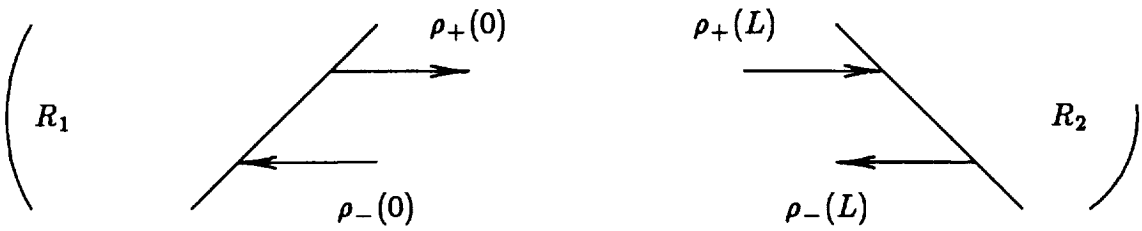

Figure 1. Geometry for photon density boundary conditions

Therefore, we require that at $z = 0$ the boundary conditions

$$\rho_+(0)\rho_-(0) = R_1\rho_-^2(0) = \frac{1}{R_1}\rho_+^2(0) = K_0. \tag{11}$$

and at $z = L$ we have the boundary condition

$$\rho_+(L)\rho_-(L) = \frac{1}{R_2}\rho_-^2(L) = R_2\rho_+^2(L) = K_0. \tag{12}$$

These conditions require that

$$\rho_+(0) = \sqrt{K_0 R_1} \qquad \text{and} \qquad \rho_+(L) = \sqrt{\frac{K_0}{R_2}}, \tag{13}$$

where R_1 and R_2 are the mirror reflectivities.

For steady state operation the initial photon density at $z = 0$ is unknown. Therefore, a shooting method is used to determine this boundary condition. That is, we first scale the above equations and introduce the variables x_7 for the density ρ_+ and y_7 for its scaled value. We then assume a value for the photon density, x_7 (or y_7), at $z = 0$ and then solve the scaled system of differential equations over the interval 0 to 1 and test the value of the photon density at the end of the laser tube by using the following arguments.

For fixed values of the reflectivities we guess at an initial value for K_0 and then integrate the system of differential equations to obtain a calculated value for $\rho_+(L)$ which is then compared with the theoretical value from equation (13). If the calculated and theoretical values are different we iterate on K_0 until the final value of $\rho_+(L)$ agrees with the theoretical value. This describes the shooting method referred to earlier. Once K_0 is determined we can use the value of the transmission coefficient given by $t_m = 1 - R_2$ and find the output power from the relation

$$P = \epsilon_\mu t_m c \rho_+(L) \quad (W/cm^2). \tag{14}$$

where ϵ_μ is the radiation energy quantum from I^* given by $\epsilon_\mu = 1.5\,(10)^{-19} \quad W\,s$.

Two Pass Amplifier

The above ideas can also be extended to model a two-pass amplifier. The geometry for the two-pass amplifier is illustrated in the figure 2.

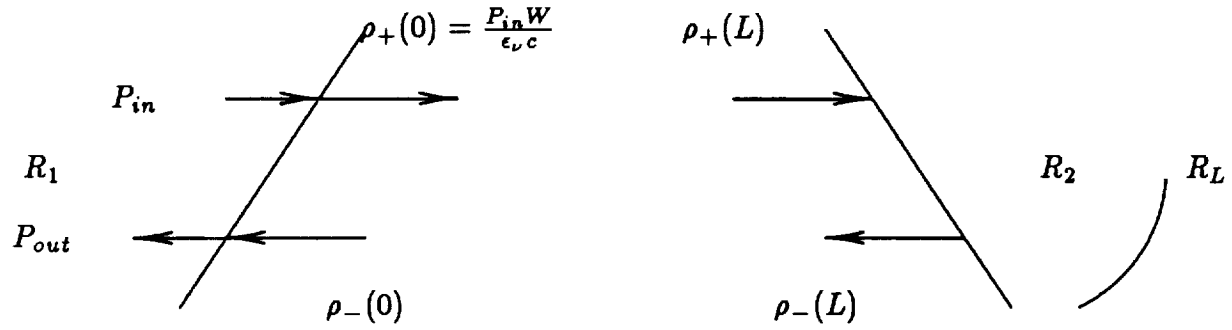

Figure 2. Geometry for Two-Pass Amplifier.

In this figure P_{in} is the power density into the amplifier $[Watts/cm^2]$, W is the transmission coefficient, ϵ_ν is the radiation energy from I^* $[Watt - sec]$, c is the speed of light, P_{out} is the output power density, R_L is the reflection coefficient of the mirror, $\rho_+(z)$ is the photon density for wave motion in the positive direction $[cm^{-3}]$, $\rho_-(z)$ is the photon density for wave motion in the negative direction $[cm^{-3}]$.

The input power density P_{in} is assumed to be known. Also the photon density satisfies for all values of z the equation (10) where K_0 is a constant. At $z = 0$ we have

$$\rho_+(0)\rho_-(0) = K_0 \tag{15}$$

and at $z = L$ we have

$$\rho_+(L)\rho_-(L) = K_0. \tag{16}$$

The value for $\rho_+(0)$ is determined from the input power density P_{in} by the relation

$$\rho_+(0) = \frac{P_{in}W}{\epsilon_\nu c} \tag{17}$$

and consequently from the relation (15) we have

$$\rho_-(0) = \frac{K_0}{\rho_+(0)}. \tag{18}$$

In the above equations W is the transmission coefficient of the Brewester windows and K_0 is an assumed initial value. At $z = L$ we have $R_2 = W^2 R_L$ as the reflection coefficient from the Brewster window. We then are able to calculate the return photon density from the Brewster window at $z = L$. We find this density has the value

$$\rho_-(L) = R_2 \rho_+(L). \tag{19}$$

Combining the equations (15),(16) and (19) we determine that

$$R_2 \rho_+^2(L) = K_0 \qquad \text{or} \qquad \rho_+(L) = \sqrt{\frac{K_0}{R_2}} = \sqrt{\frac{\rho_+(0)\rho_-(0)}{R_2}}. \tag{20}$$

Using the value given by equation (20) as a theoretical value for $\rho_+(L)$ we can compare this value with the calculate value for $\rho_+(L)$ obtained from an integration of the differential equations defining the chemical reactions occurring in the amplifier. We adjust the value for $\rho_(0)$ (by adjusting K_0) until

$$|\rho_+(L)_{theoretical} - \rho_+(L)_{calculated}| < E \tag{21}$$

where E is an error criteria. The above procedure is again a shooting method for the determination of $\rho_-(0)$. When the error criteria is satisfied, the output power is obtainable from the relation

$$P_{out} = \rho_(0) W \epsilon_\nu C \tag{22}$$

and the gain is calculated from the relation

$$gain = 10 \, \mathrm{Log}_{10} \left(\frac{P_{out}}{P_{in}} \right) \quad \text{[decibels]}. \tag{23}$$

Again the length of the amplifier is normalized to unity and the system of differential equations are solved using a Runge-Kutta integration scheme. Previous progress reports have the computer codes for both the iodine laser and the amplifier models.

In both the iodine and amplifier models the compressibility of the perflouride gas requires additional considerations. If the perflouroalkyl iodide gas is incompressible the above equations hold. For a compressible gas we must add to the above equations an equation of state, a continuity equation, a momentum equation and an energy equation.

COMPRESSIBILITY EFFECTS

Equation of State

We assume an equation of state for an ideal gas and write

$$P = \eta RT \tag{15}$$

where P is the gas pressure $[Pa]$, η is the gas density $[Kg/m^3]$, T is the absolute temperature $[K]$, and $R = R^*/M$ $[J/Kg\,K]$ with M the mass of the gas and R^* is the gas constant, $R^* = 8.317\,[J/mole\,K]$. For $n - C_3F_7I$ we use the value $M = 296\,Kg/mole$ and for $t - C_4F_9I$ we use the value $M = 346\,Kg/mole$ to convert R^* to R.

Continuity Equation

The continuity equation expressing the conservation of mass flow can be represented

$$\frac{\partial \eta}{\partial t} + \text{div}\,(\eta \vec{V}) = 0 \tag{16}$$

where η is the fluid density $[Kg/m^3]$, and $\vec{V}$ is the fluid velocity $[m/s]$. For steady state conditions and a flow in the axial direction we let $\vec{V} = \omega\,\hat{k}$ and reduce the continuity equation to the form

$$\frac{\partial}{\partial z}(\eta\omega) = 0.$$

An integration of this equation gives

$$\eta\,\omega = C_1 = Constant, \tag{17}$$

where C_1 is a constant of integration.

Momentum Equation

The momentum equation for a control volume having a mass $\eta d\tau$, where $d\tau$ is an element of volume, is given by

$$\vec{M} = \iiint \vec{V}\eta \, d\tau.$$

Using Newton's second law we write

$$\vec{F} = \frac{D\vec{M}}{Dt} = \frac{D}{Dt}\iiint \vec{V}\eta \, d\tau \tag{18}$$

where, D/Dt is the material derivative. Consequently, we find

$$\frac{D\vec{M}}{Dt} = \iint \vec{V}(\eta\vec{V}\, d\vec{\sigma}) + \frac{\partial}{\partial t}\iiint \vec{V}\eta \, d\tau \tag{19}$$

where $d\vec{\sigma}$ is a vector element of surface area. The surface integral term in equation (18) represents the efflux of momentum through the control volume and the volume integral term in equation (18) represents the change in momentum inside the control volume. Using the Gauss divergence theorem, we can change the surface integral to a volume integral and write

$$\iint_S \vec{V}(\eta\vec{V}\, d\vec{\sigma}) = \iiint_V \left[\nabla \cdot \eta\vec{V}\vec{V}\right] d\tau. \tag{20}$$

Then the momentum equation becomes

$$\vec{F} = \frac{D\vec{M}}{Dt} = \iiint \mathrm{div}(\eta\vec{V}\vec{V})\, d\tau + \frac{\partial}{\partial t}\iiint (\eta\omega\,\hat{k})\, d\tau \tag{21}$$

where $\vec{V}\vec{V}$ is the dyadic $\omega^2\,\hat{k}\hat{k}$ of $\vec{V} = \omega\,\hat{k}$, and

$$\nabla \cdot \eta\vec{V}\vec{V} = \frac{\partial}{\partial z}(\eta\omega^2)\,\hat{k}. \tag{22}$$

We also make the substitutions $\vec{F} = \iiint \vec{f}\, d\tau$ where $\vec{f}$ is the average force per unit volume as this allows the momentum equation to be written in the form

$$\vec{F} = \iiint \vec{f}\, d\tau = \frac{D\vec{M}}{Dt} = \iiint \left[\frac{\partial}{\partial t}(\eta\omega)\,\hat{k} + \frac{\partial}{\partial z}(\eta\omega^2)\,\hat{k} \right] d\tau \tag{23}$$

Neglecting the viscosity and using $\vec{f} = -\nabla P$ as the average force per unit volume (which is due to the fluid pressure P), we have

$$-\frac{\partial P}{\partial z} = \frac{\partial}{\partial t}(\eta\omega) + \frac{\partial}{\partial z}(\eta\omega^2) \tag{24}$$

From the equation (17) we use $\eta\omega = C_1$ and examine the steady state form of the equation (22) to obtain

$$-\frac{\partial P}{\partial z} = C_1 \frac{\partial \omega}{\partial z}. \tag{25}$$

Integrating the equation (25) produces the result

$$P + C_1\omega = C_2, \tag{26}$$

where C_2 is a constant of integration.

Energy Equation

In terms of the specific enthalpy h per unit mass, the energy equation for the fluid flow is

$$\eta \frac{Dh}{Dt} = \frac{DP}{Dt} + \kappa\nabla^2 T + q \tag{27}$$

where P is the pressure, T is the absolute temperature, κ is the thermal conductivity and $q = q(z)$ is the radiation heat flux. In one dimension the equation (25) reduces to

$$\eta \frac{\partial h}{\partial t} + \eta\omega \frac{\partial h}{\partial z} = \frac{\partial P}{\partial t} + \omega \frac{\partial P}{\partial z} + \kappa \frac{d^2 T}{dz^2} + q. \tag{28}$$

The specific enthalpy h can be expressed in terms of the specific heat at constant pressure and

$$h = C_p T. \tag{29}$$

Using the relation

$$C_p^* - C_v^* = R^* \tag{30}$$

the specific heat at constant pressure C_p^* can be expressed in terms of the specific heat at constant volume C_v^* and the universal gas constant R^*, where $R^* = 8.317\,[J/moleK]$. We use the following numerical data to obtain a least squares approximation for the specific heat at constant volume.

$Temperature(K)$	298.15	400.00	500.00
C_v for $n - C_3F_7I\,[J/mole\,K]$	146	169	186
C_v for $t - C_4F_9I\,[J/mole\,K]$	181	215	240

Using least squares there results the approximations

$$C_v = 183.26\exp(0.0014(T-300)) \qquad \text{for } t - C_4F_9I$$

$$C_v = 147.23\exp(0.0012(T-300)) \qquad \text{for } n - C_3F_7I$$

Stimulated Emission Cross-Section

The stimulated emission cross-section is given by (references 6,7 and 8)

$$\sigma_{ij} = \frac{\lambda^2 A_{ij}}{8\pi} g_{ij}(\nu) \tag{31}$$

where, $g_{ij}(\nu)$ is the normalized line shape function

$$g_{ij}(\nu) = \frac{2}{\pi\,\delta\nu\left(1 + 4\left[\frac{\nu-\nu_{ij}}{\delta\nu}\right]^2\right)} \tag{32}$$

The level transitions for the iodine laser are illustrated in the figure 3. The relative intensities of these transitions are illustrated in the figure 4. The Einstein coefficients for the different lines have the transition rates

$$\begin{aligned} A_{34} &= 5.0\alpha \qquad A_{23} = 2.3\alpha \\ A_{33} &= 2.1\alpha \qquad A_{22} = 3.0\alpha \\ A_{32} &= 0.6\alpha \qquad A_{21} = 2.4\alpha \end{aligned} \tag{33}$$

in units of $\sec^-1$, where $\alpha = A/7.77$ with $A = 5.4 \pm 2.0\,\sec^-1$. Using

$$\nu_0 = \frac{c}{1.315246\,(10)^{-4}} = 2.28094\,(10)^{14} \approx 2.3\,(10)^4\,\text{GHz} \tag{34}$$

the laser emission frequencies from ν_0 are given by

$$\begin{aligned} \nu_{34} &= \nu_0 \qquad & \nu_{21} &= \nu_0 - 0.427c \\ \nu_{33} &= \nu_0 + 0.141c \qquad & \nu_{22} &= \nu_{21} - 0.026c \\ \nu_{32} &= \nu_{33} + 0.068c \qquad & \nu_{23} &= \nu_{22} - 0.068c \end{aligned} \tag{35}$$

and consequently the overall stimulated emission cross-section is given by

$$\sigma = \frac{\lambda^2}{4\pi^2 \delta\nu} \left[\frac{5}{12} \sum_{i=1}^{3} \frac{A_{2i}}{1 + \left[2\left(\frac{\nu - \nu_{2i}}{\delta\nu}\right)\right]^2} + \frac{7}{12} \sum_{i=2}^{4} \frac{A_{3i}}{1 + \left[2\left(\frac{\nu - \nu_{3i}}{\delta\nu}\right)\right]^2} \right] \tag{36}$$

which is based upon the statistical weights of the hyperfine levels (reference 1) and

$$\delta\nu = \alpha_0 + \alpha_1 p \tag{37}$$

with $\alpha_0 = 2.51\,(10)^8 \sqrt{T/300}$, $\alpha_1 = 1.88\,(10)^7 \sqrt{T/300}$ where p is the pressure in torr, and T is the absolute temperature. Here α_0 is related to the Doppler line width and α_1 is the pressure broadening coefficient associated with the lasant $n - C_3F_7I$.

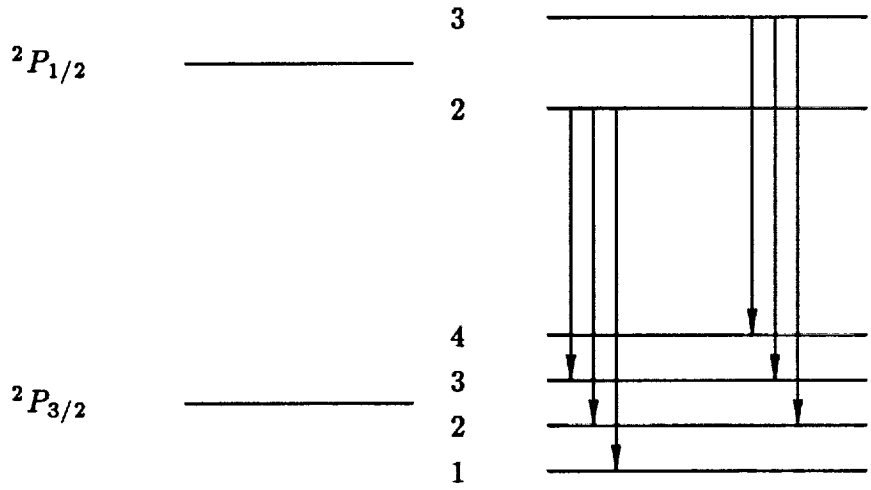

Figure 3. Level transitions for iodine

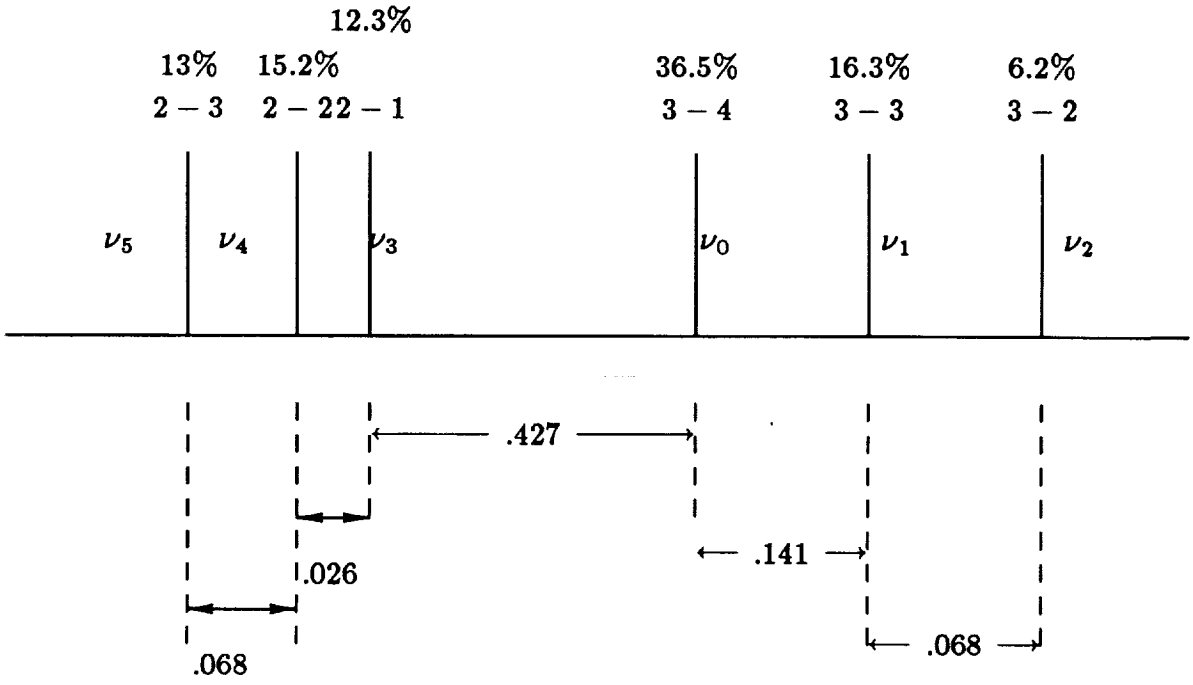

Figure 4 Relative intensities for iodine transitions

The figures 5,6,7,8 contain graphs of the stimulated emission cross-section for various pressures.

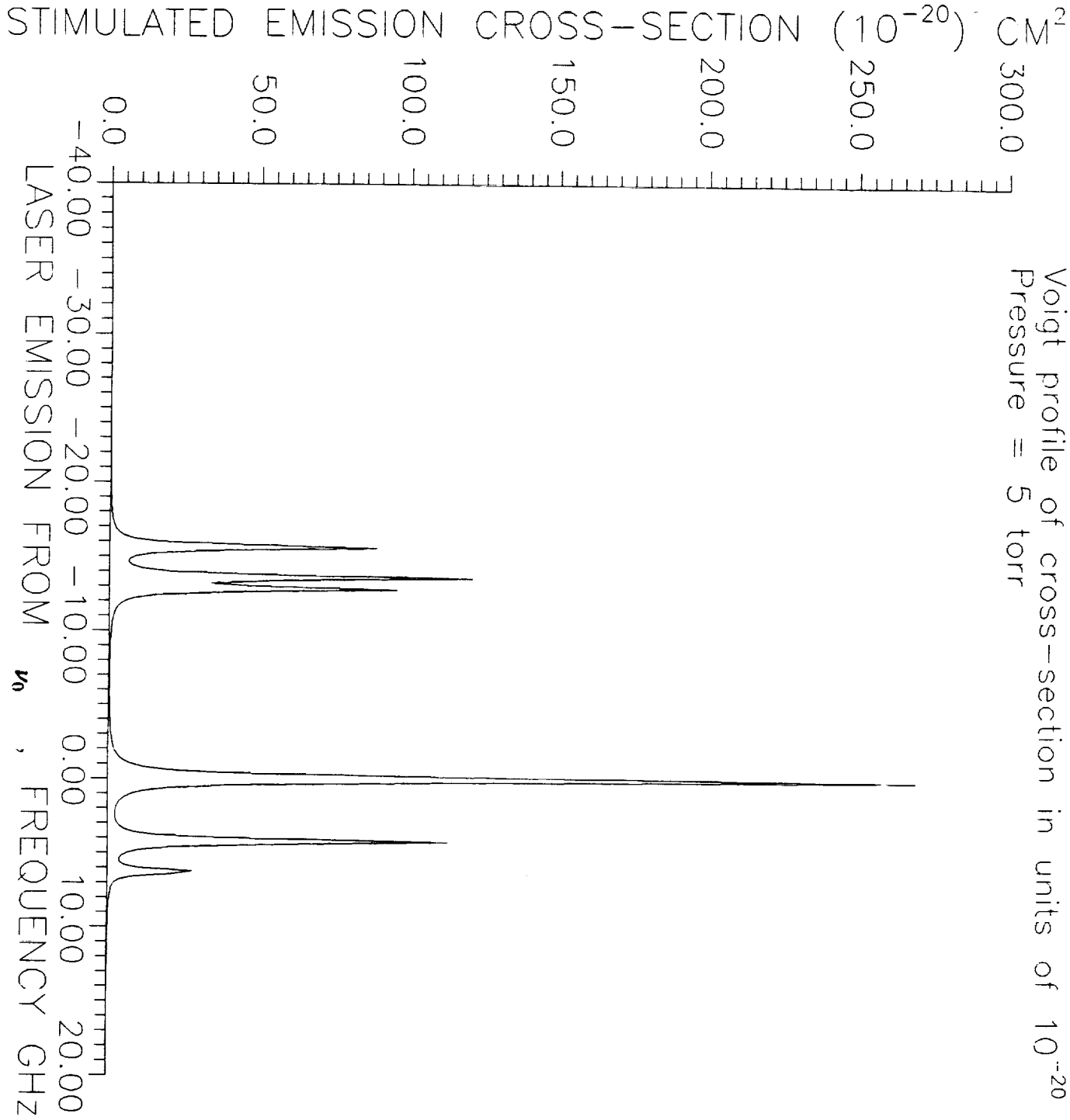

Figure 5 Stimulated emission cross-section $(10)^{-20}$ cm^2 vs laser emission from ν_0, frequency GHz with pressure of 5 torr

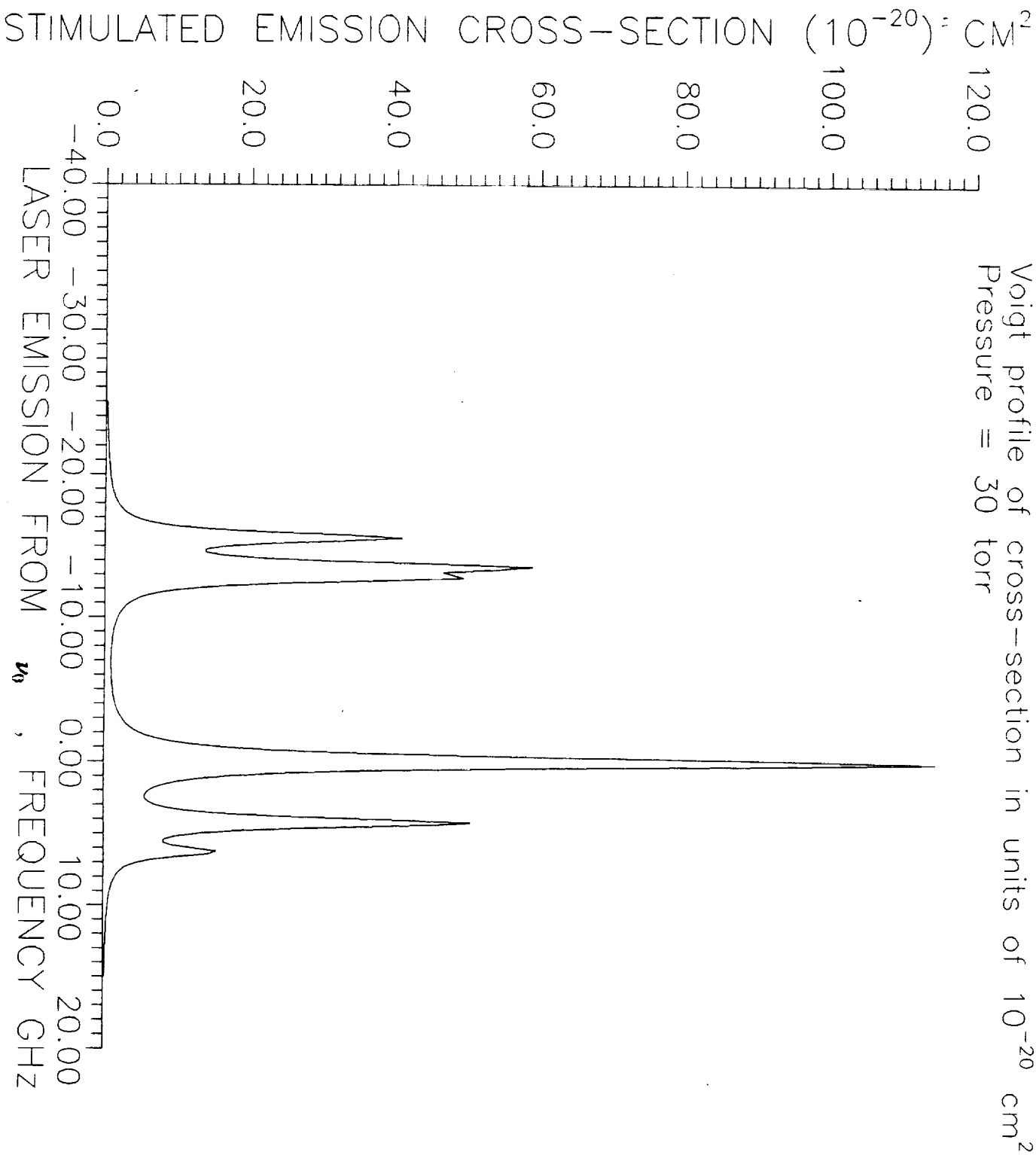

Figure 6 Stimulated emission cross-section $(10)^{-20}$ cm^2 vs laser emission from ν_0, frequency GHz with pressure of 30 torr

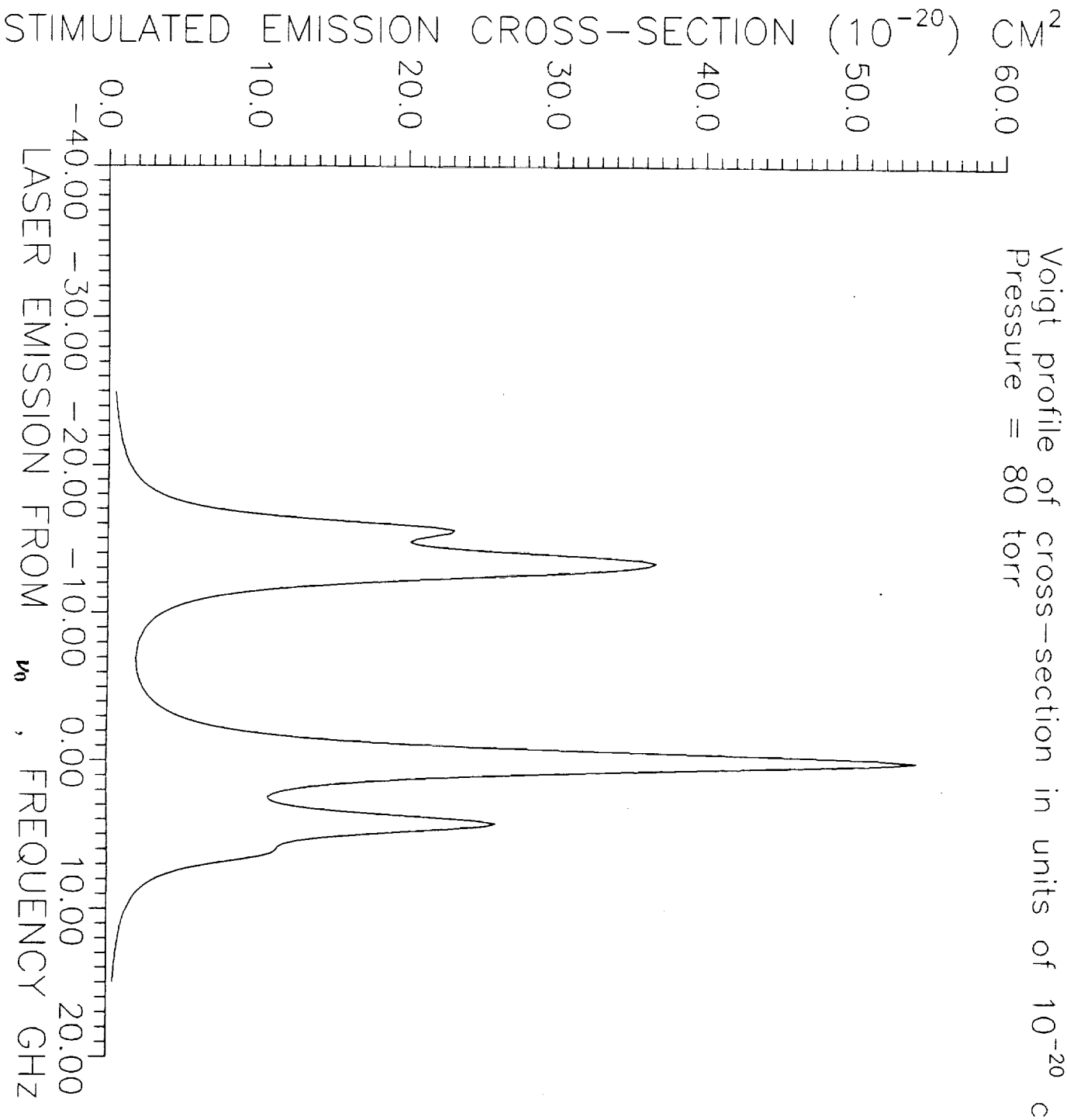

Figure 7 Stimulated emission cross-section $(10)^{-20}$ cm^2 vs laser emission from ν_0, frequency GHz with pressure of 80 torr

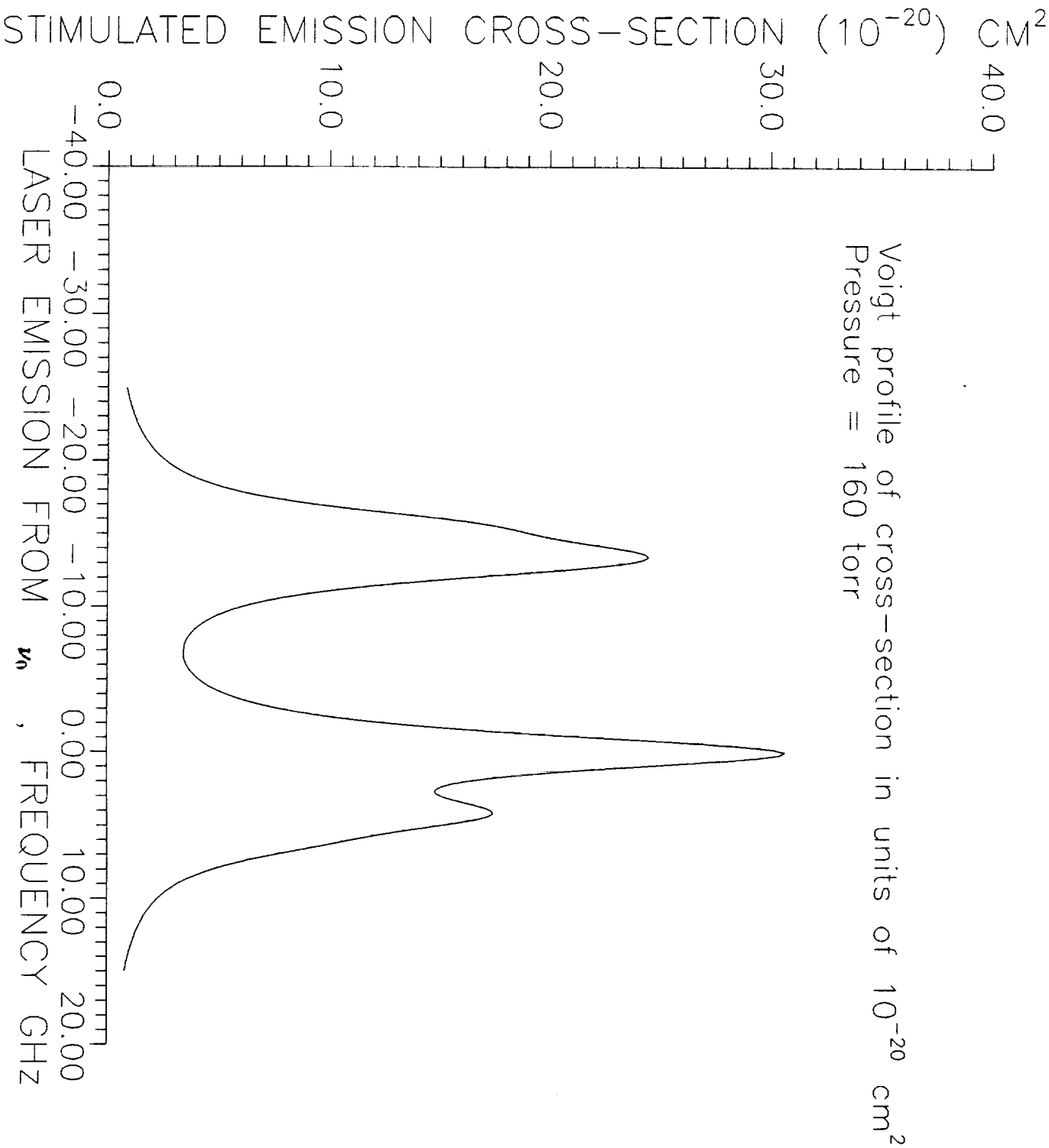

Figure 8 Stimulated emission cross-section $(10)^{-20}$ cm^2 vs laser emission from ν_0, frequency GHz with pressure of 160 torr

The above models were used to compare theoretical output with results from various laboratory experiments. It was found that certain of the reaction rate coefficients had to be changed in order to make theory agree with experiment. Additional experimental results indicated that the purity of the iodide gases was in question and so we felt justified in varying some of the reaction rate coefficients. The Appendix A contains a sampling of the various theoretical results obtained during the course of this study.

Bibliography

[1] John W. Wilson, S. Raja, Y.J. Shiu, Solar-Simulator-Pumped Atomic Iodine Laser Kinetics, NASA Technical Paper 2182, August 1983.

[2] John W. Wilson, Yeunggil Lee, Willard R. Weaver, Donald H. Humes, Ja H. Lee, Threshold Kinetics of a Solar-Simulator-Pumped Iodine Laser, NASA Technical Paper 2241, February 1984.

[3] L.V. Stock, J.W. Wilson, R.J. DeYoung, A model for the Kinetics of a Solar-Pumped Long Path Laser Experiment, NASA Technical Memorandum 87668, May 1986.

[4] J.S. Cohen, O.P. Judd, High Energy Optically Pumped Iodine Laser I. Kinetics in an Optically Thich Medium., J. Appl. Phys. 55(7), 1 April 1984.

[5] E.V. Arkhipova, B.L. Borovich, A.K. Zapalskii, Accumulation of Excited Iodine Atoms in Iodine Photodissociation Laser. Analysis of Kinetic Equations., Sov. J. Quantum Electron. , Vol 6, No.6, June 1976.

[6] G. Breederlow, E. Fill, K.J. White, **The High-Power Iodine Laser**, Springer-Verlag, Berlin, Heidelberg, New York, 1983.

[7] P.W. Milonni, J.A. Eberly, **Lasers**, John Wiley & Sons, 1988.

[8] J.T. Verdeyen, **Laser Electronics**, Prentice-Hall, 1989.

APPENDIX A

Miscellaneous Results

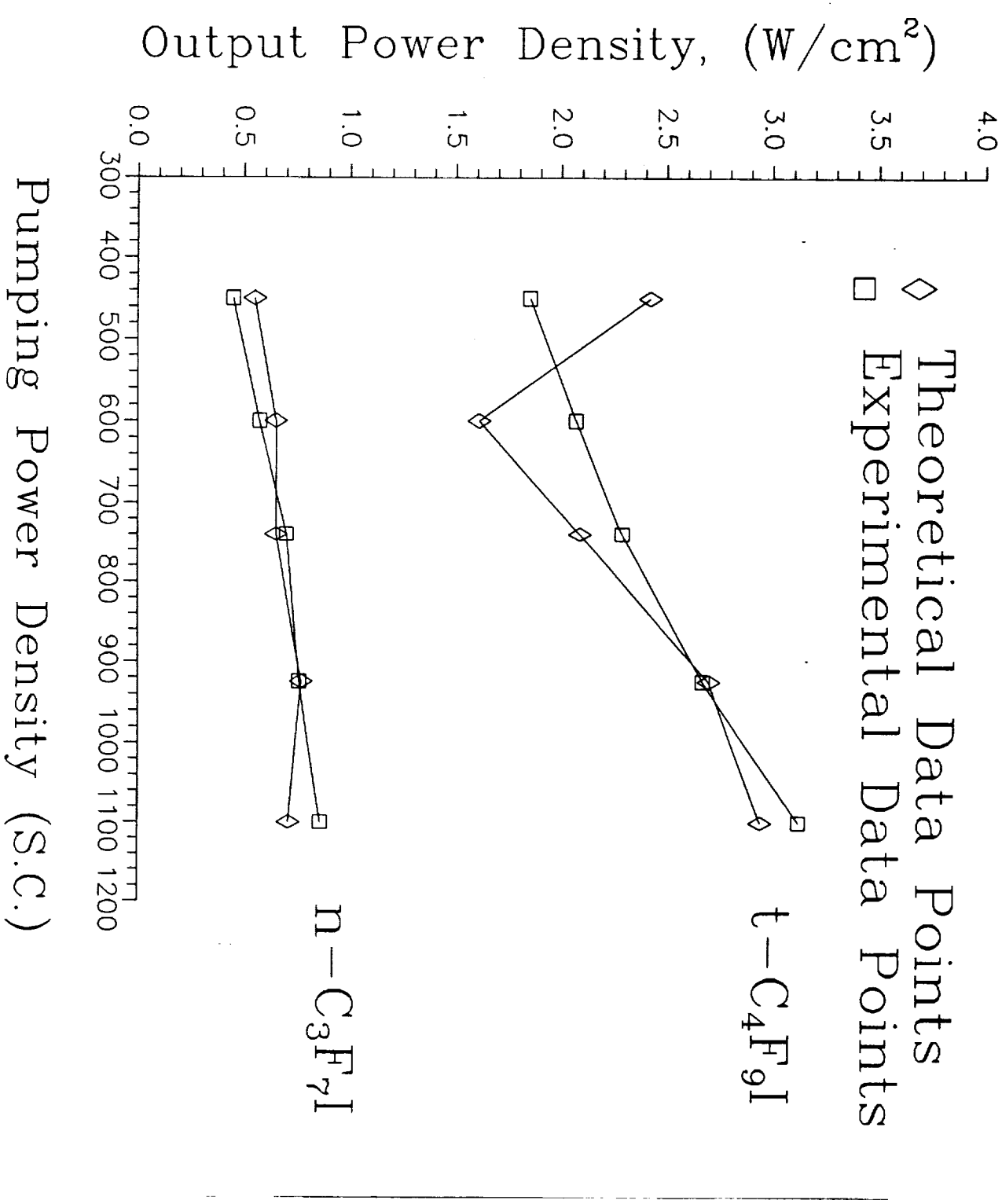

Figure A1 Parameter Fit of $t - C_4F_9I$ and $n - C_3F_7I$ data

n-C3F7I		t-C4F9I	
PT0 =	5.600E+00	PT0 =	9.00E+00
OMEG1 =	6.630E+02	OMEG1 =	5.50E+02
C00 =	1.000E+17	C00 =	1.40E+19
R1 =	1.000E+00	R1 =	1.00E+00
R2 =	7.000E-01	R2 =	7.00E-01
TM =	3.000E-01	TM =	3.00E-01
XNRHO =	1.000E+00	XNRHO =	1.00E+00
CON =	4.500E+02	CON =	4.50E+02
LC =	3.300E+01	LC =	3.30E+01
ZOL =	7.500E+00	ZOL =	7.50E+00
A =	1.000E+00	A =	1.00E+00
R20 =	0.000E+00	R20 =	0.00E+00
FRAC =	3.750E-04	FRAC =	3.75E-04
T0 =	3.000E+02	T0 =	3.00E+02
RAD =	0.000E+00	RAD =	0.00E+00
V1 =	0.000E+00	V1 =	0.00E+00
V2 =	0.000E+00	V2 =	0.00E+00
TTT2 =	1.000E+18	TTT2 =	1.00E+18
TTT3 =	1.000E+18	TTT3 =	1.00E+18
TTT4 =	1.000E+18	TTT4 =	1.00E+18
TTT5 =	1.000E+18	TTT5 =	1.00E+18
TTT6 =	1.000E+18	TTT6 =	1.00E+18
CHI1 =	1.200E-02	CHI1 =	1.44E-02
CHI2 =	1.200E-01	CHI2 =	1.20E-01
CHI3 =	0.000E+00	CHI3 =	0.00E+00
KK1 =	1.000E-14	KK1 =	1.00E-14
KK2 =	2.300E-11	KK2 =	6.00E-12
KK3 =	2.000E-12	KK3 =	3.00E-14
KK4 =	3.000E-16	KK4 =	3.00E-18
KK5 =	1.000E-11	KK5 =	1.00E-11
KK6 =	0.000E+00	KK6 =	0.00E+00
KK7 =	3.000E-19	KK7 =	3.00E-19
KK8 =	1.600E-23	KK8 =	1.60E-23
KK9 =	1.000E+15	KK9 =	1.00E+14
KK10 =	1.000E+17	KK10 =	1.00E+16
AA0 =	1.472E+02	AA0 =	1.83E+02
BB0 =	1.200E-03	BB0 =	1.40E-03
CC1 =	1.600E-33	CC1 =	1.60E-33
CC2 =	5.700E-33	CC2 =	5.70E-33
CC3 =	0.000E+00	CC3 =	0.00E+00
CC4 =	1.000E+00	CC4 =	1.00E+00
CC5 =	8.000E-33	CC5 =	8.00E-33
QQ1 =	1.700E-17	QQ1 =	6.10E-17
QQ2 =	2.890E-11	QQ2 =	2.89E-11
QQ3 =	3.700E-18	QQ3 =	3.70E-18
QQ4 =	4.700E-16	QQ4 =	4.70E-16
QQ5 =	1.600E-14	QQ5 =	1.60E-14
WTMOL =	2.960E+02	WTMOL=	3.46E+02

Table A1 Parameter Values for Figure A1

n-C3F7I

P	Con	Omega	Power Density w/cm*cm	
torr	S.C.	cm/sec	Calculated	Experimental
5.6	450.0	663.0	0.550	0.450
5.6	600.0	663.0	0.650	0.573
6.0	740.0	619.0	0.650	0.700
5.8	925.0	640.0	0.770	0.760
6.4	1100.0	580.0	0.710	0.860

t-C4F9I

P	Con	Omega	Power Density	
9.0	450.0	550.0	2.420	1.850
4.5	600.0	733.0	1.610	2.070
4.5	740.0	733.0	2.090	2.290
4.5	925.0	707.0	2.700	2.670
4.2	1100.0	707.0	2.940	3.120

Table B1 Data for Figure A1

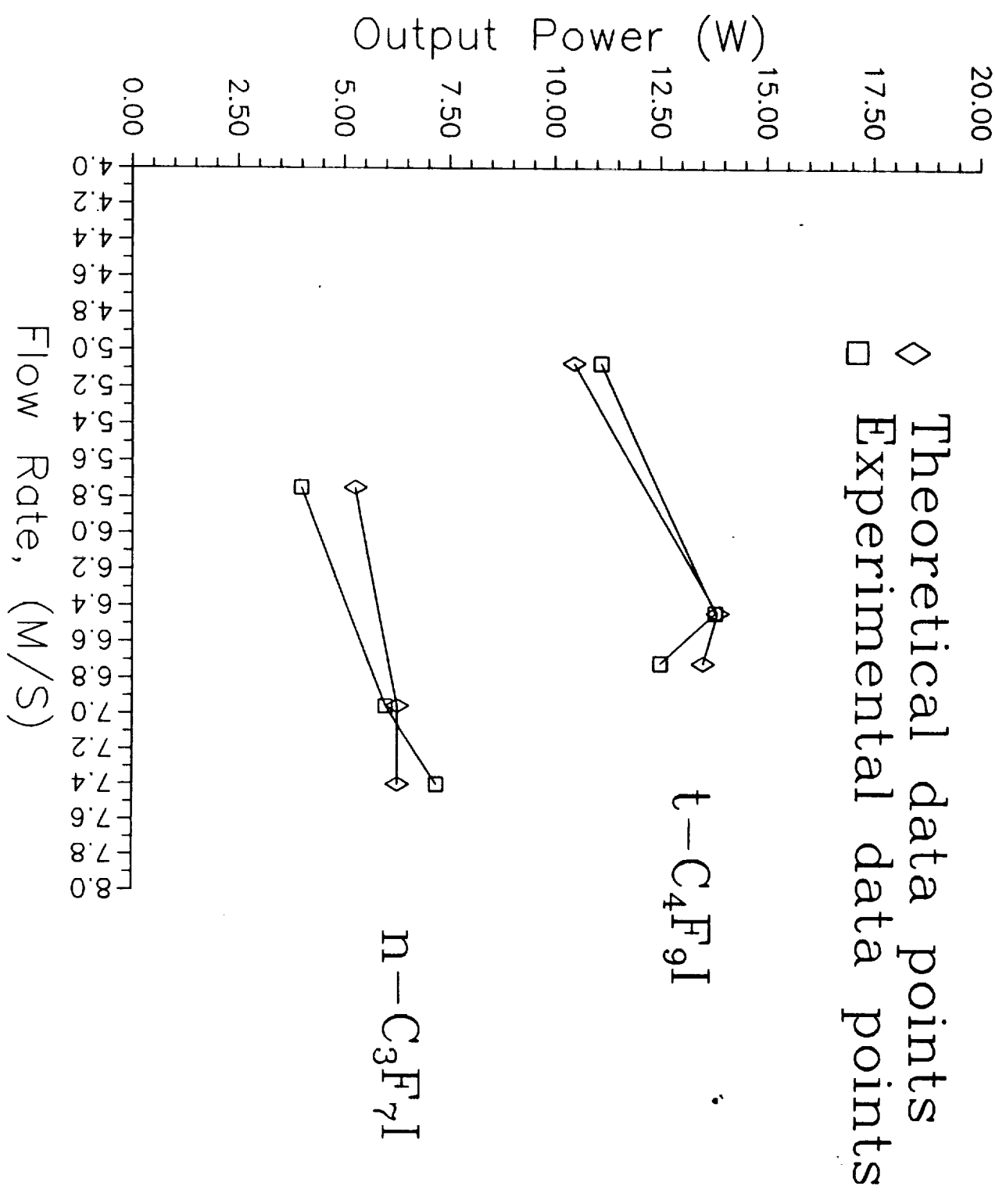

Figure A2(a) Parameter fit of $t - C_4F_9I$ and $n - C_3F_7I$ data (Flow Rate (M/S) Vs Power)

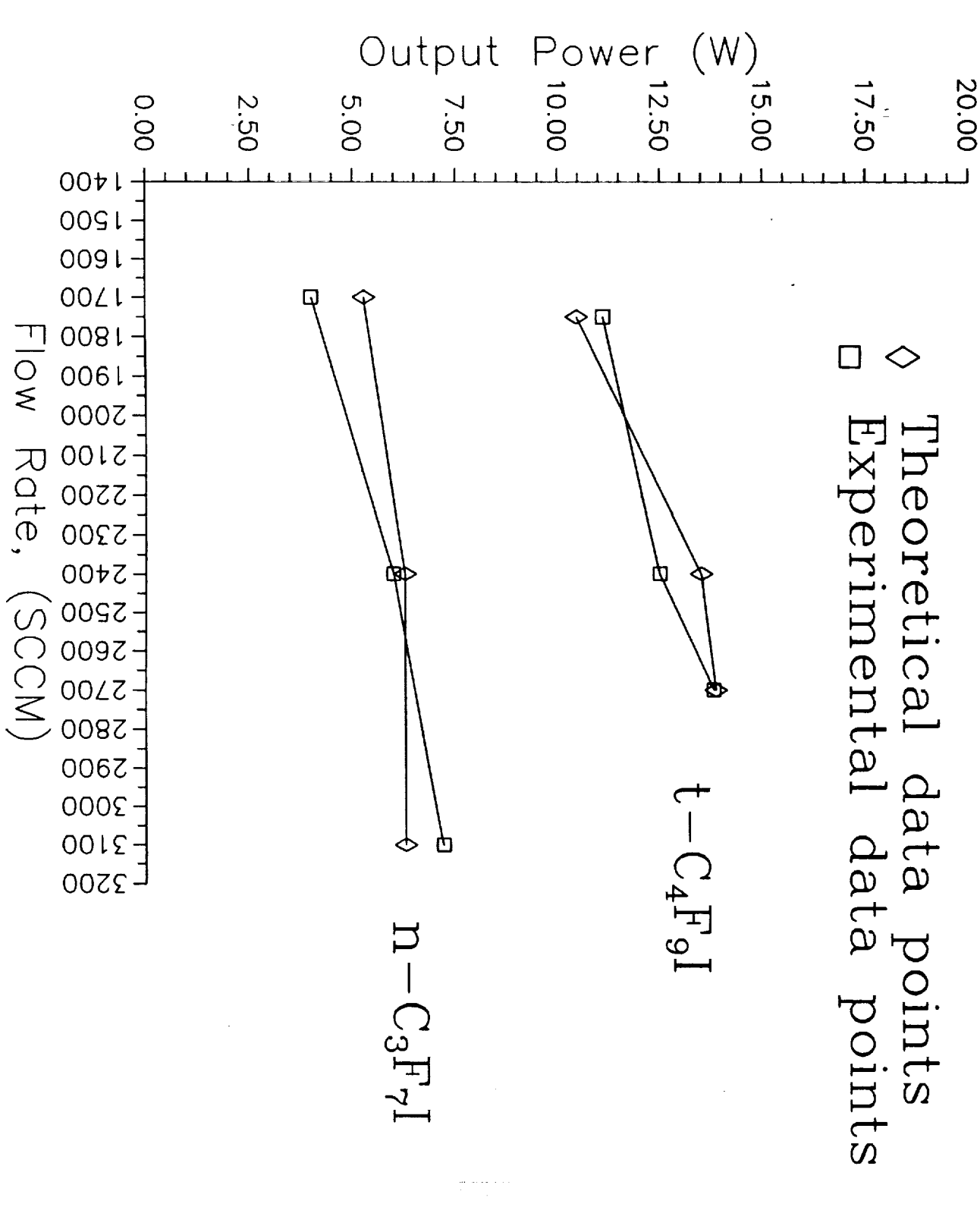

Figure A2(b) Parameter Fit of $t - C_4F_9I$ and $n - C_3F_7I$ data (Flow Rate (SCCM) Vs Power

	n-C3F7I		t-C4F9I
PT0 =	17.000000	PT0 =	17.000000
OMEG1 =	740.100000	OMEG1 =	644.60000
C00 =	8.500000E+17	C00 =	6.150000E+18
R1 =	1.000000	R1 =	1.000000
R2 =	6.750000E-01	R2 =	6.750000E-01
TM =	3.250000E-01	TM =	3.250000E-01
XNRHO =	1.000000	XNRHO =	1.00000
CON =	1000.000000	CON =	1000.000000
LC =	33.000000	LC =	33.000000
ZOL =	7.500000	ZOL =	7.500000
A =	1.000000	A =	1.000000
R20 =	0.000000E+00	R20 =	0.000000E+00
FRAC =	1.000000E-03	FRAC =	1.000000E-03
T0 =	300.000000	T0 =	300.000000
RAD =	0.000000E+00	RAD =	0.000000E+00
V1 =	0.000000E+00	V1 =	0.000000E+00
V2 =	0.000000E+00	V2 =	0.000000E+00
TTT2 =	1.000000E+18	TTT2 =	1.000000E+18
TTT3 =	1.000000E+18	TTT3 =	1.000000E+18
TTT4 =	1.000000E+18	TTT4 =	1.000000E+18
TTT5 =	1.000000E+18	TTT5 =	1.000000E+18
TTT6 =	1.000000E+18	TTT6 =	1.000000E+18
CHI1 =	1.200000E-02	CHI1 =	1.440000E-02
CHI2 =	1.200000E-01	CHI2 =	1.200000E-01
CHI3 =	0.000000E+00	CHI3 =	0.000000E+00
KK1 =	1.000000E-14	KK1 =	1.000000E-14
KK2 =	8.800000E-11	KK2 =	8.800000E-11
KK3 =	2.000000E-12	KK3 =	3.000000E-13
KK4 =	3.000000E-16	KK4 =	3.000000E-17
KK5 =	1.000000E-11	KK5 =	1.000000E-11
KK6 =	0.000000E+00	KK6 =	0.000000E+00
KK7 =	3.000000E-19	KK7 =	3.000000E-19
KK8 =	1.600000E-23	KK8 =	1.600000E-23
KK9 =	1.000000E+15	KK9 =	1.000000E+14
KK10 =	1.000000E+17	KK10 =	1.000000E+16
AA0 =	147.230000	AA0 =	183.262400
BB0 =	1.200000E-03	BB0 =	1.398681E-03
CC1 =	1.600000E-33	CC1 =	1.600000E-33
CC2 =	5.700000E-33	CC2 =	5.700000E-33
CC3 =	0.000000E+00	CC3 =	0.000000E+00
CC4 =	1.000000	CC4 =	1.000000
CC5 =	8.000000E-33	CC5 =	8.000000E-33
QQ1 =	1.700000E-17	QQ1 =	6.100000E-17
QQ2 =	2.890000E-11	QQ2 =	2.890000E-11
QQ3 =	3.700000E-18	QQ3 =	3.700000E-18
QQ4 =	4.700000E-16	QQ4 =	4.700000E-16
QQ5 =	1.600000E-14	QQ5 =	1.600000E-14
WTMOL =	296.000000	WTMOL =	346.00000

Table A2 Parameter Values for Figures A2(a)(b)

n-C3F7I

p Torr	Con S.C.	Omega cm/sec	Power (W) Calculated	Power(W) Experimental	SCCM
12.0	1000	574.9	5.28	4.00	1700
14.0	1000	695.7	6.28	6.00	2400
17.0	1000	740.1	6.28	7.20	3100

t-C4F9I

p Torr	Con S.C.	Omega cm/sec	Power (W) Calculated	Power(W) Experimental	SCCM
14.0	1000	507.3	10.46	11.1	1750
14.5	1000	671.7	13.85	12.5	2400
17.0	1000	644.6	13.51	13.8	2700

n-C3F7I

p Torr	Con S.C.	Omega cm/sec	Power (W) Calculated	Power(W) Experimental	SCCM
12.0	1000	574.9	5.28	4.00	1700
14.0	1000	695.7	6.28	6.00	2400
17.0	1000	740.1	6.28	7.20	3100

t-C4F9I

p Torr	Con S.C.	Omega cm/sec	Power (W) Calculated	Power(W) Experimental	SCCM
14.0	1000	507.3	10.46	11.1	1750
14.5	1000	671.7	13.85	12.5	2400
17.0	1000	644.6	13.51	13.8	2700

Table B2 Data for Figures A2(a)(b)

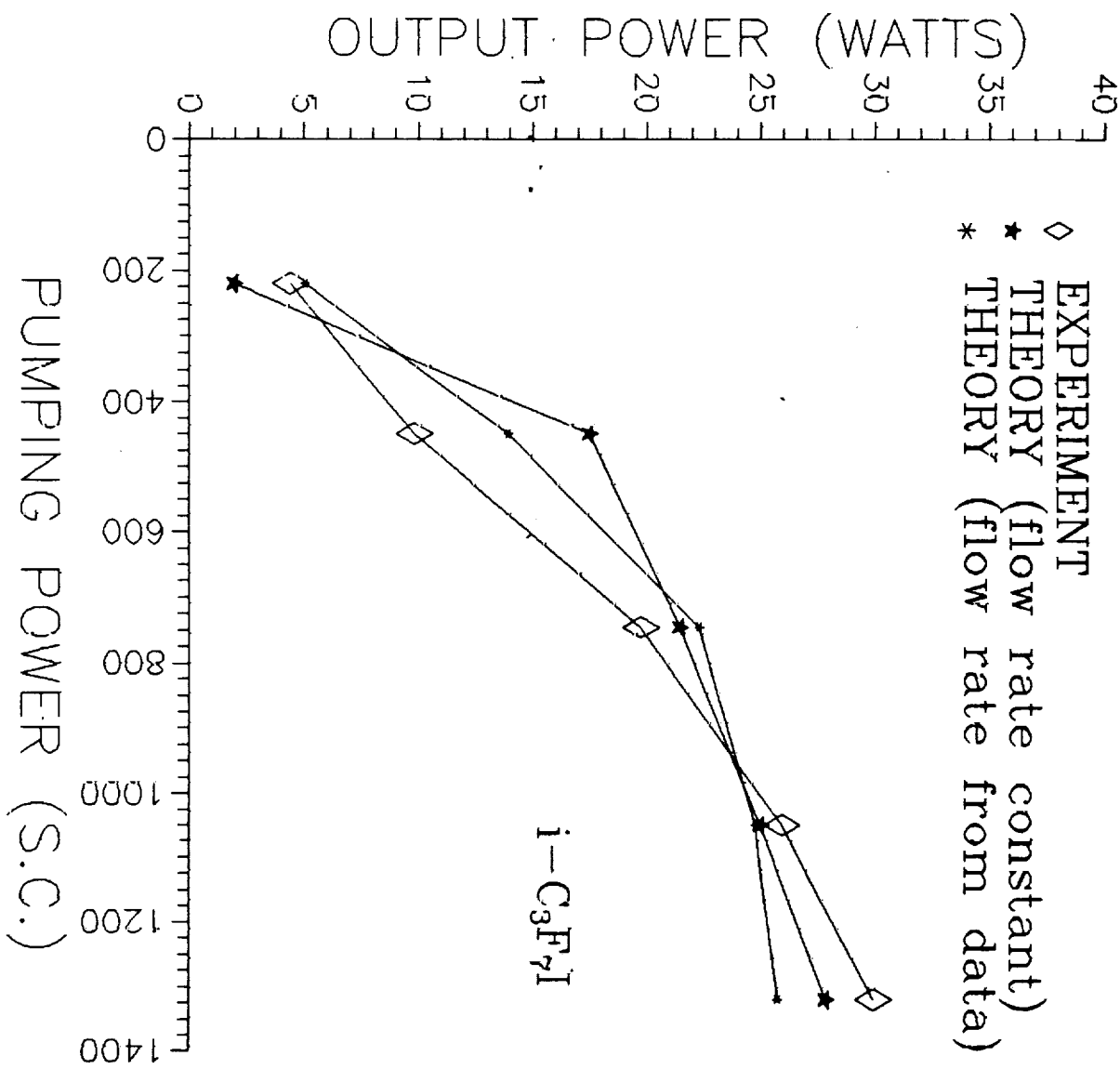

Figure A3(a) Parameter Fit for $i - C_3F_7I$ data

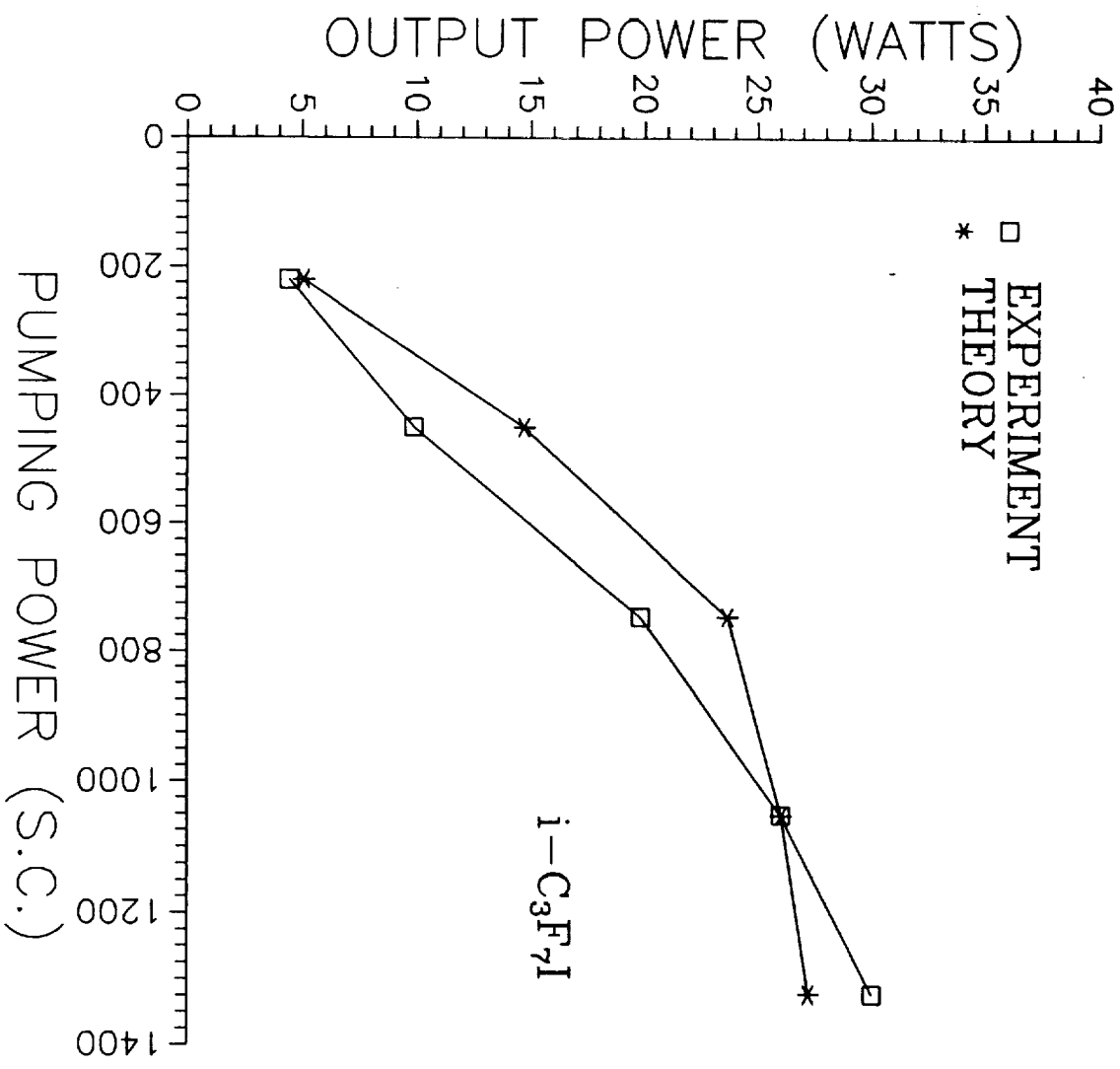

Figure A3(b) Parameter Fit for $i - C_3F_7I$ data

```
&PARAM
PT0 =          3.580000
OMEG1 =        363.200000
C00 =      3.900000E+18
R1 =           1.000000
R2 =       8.500000E-01
TM =       1.500000E-01
XNRHO =            1.000000
CON =        220.000000
LC =         15.000000
ZOL =          7.500000
A =            1.850000
R20 =      0.000000E+00
FRAC =      4.500000E-04
T0 =         300.000000
RAD =      0.000000E+00
V1 =       0.000000E+00
V2 =       0.000000E+00
TTT2 =       1.000000E+18
TTT3 =       1.000000E+18
TTT4 =       1.000000E+18
TTT5 =       1.000000E+18
TTT6 =       1.000000E+18
CHI1 =       1.200000E-02
CHI2 =       1.200000E-01
CHI3 =       0.000000E+00
KK1 =       1.000000E-14
KK2 =       2.300000E-11
KK3 =       6.500000E-13
KK4 =       3.000000E-16
KK5 =       5.000000E-11
KK6 =       0.000000E+00
KK7 =       3.000000E-19
KK8 =       1.600000E-23
KK9 =       1.000000E+15
KK10 =       1.000000E+17
AA0 =          147.230000
BB0 =       1.200000E-03
CC1 =       1.600000E-33
CC2 =       5.700000E-33
CC3 =       0.000000E+00
CC4 =            1.000000
CC5 =       8.000000E-33
QQ1 =       1.700000E-17
QQ2 =       2.890000E-11
QQ3 =       3.700000E-18
QQ4 =       4.700000E-16
QQ5 =       1.600000E-14
/
```

CON	POWER(W) (THEORY)	POWER(W) (CALCULATED)
220	4.42	5.05
450	9.86	14.7
745	19.8	23.65
1050	26.0	26.02
1320	30.0	27.2

Table A3 Data for Figures A3(a)(b)

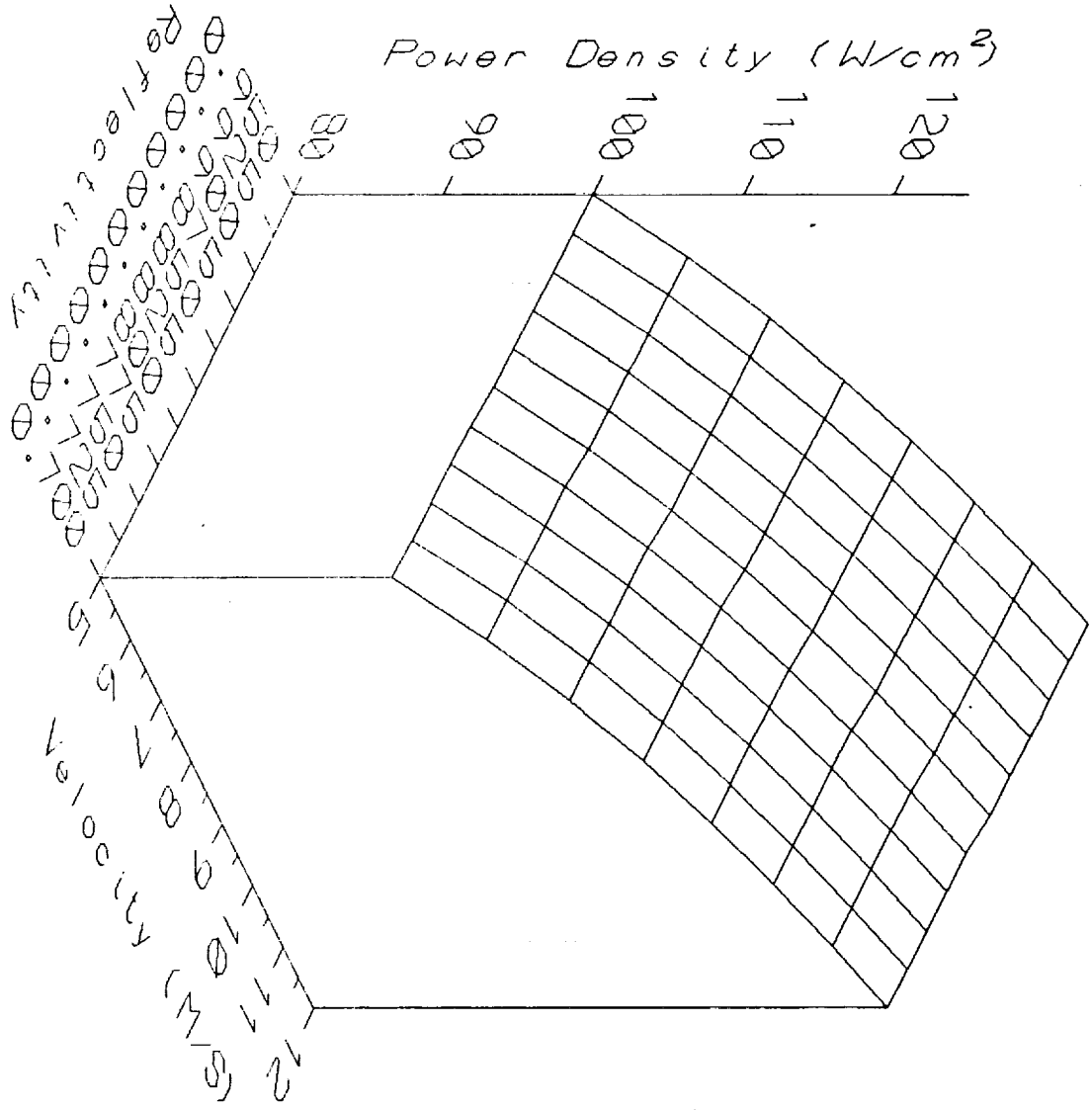

$L = 500\,\text{cm}$ $a = 15\,\text{cm}$ $frac = 0.0005$

Figure A4(a) Simulated $t - C_4F_9$ Space Laser

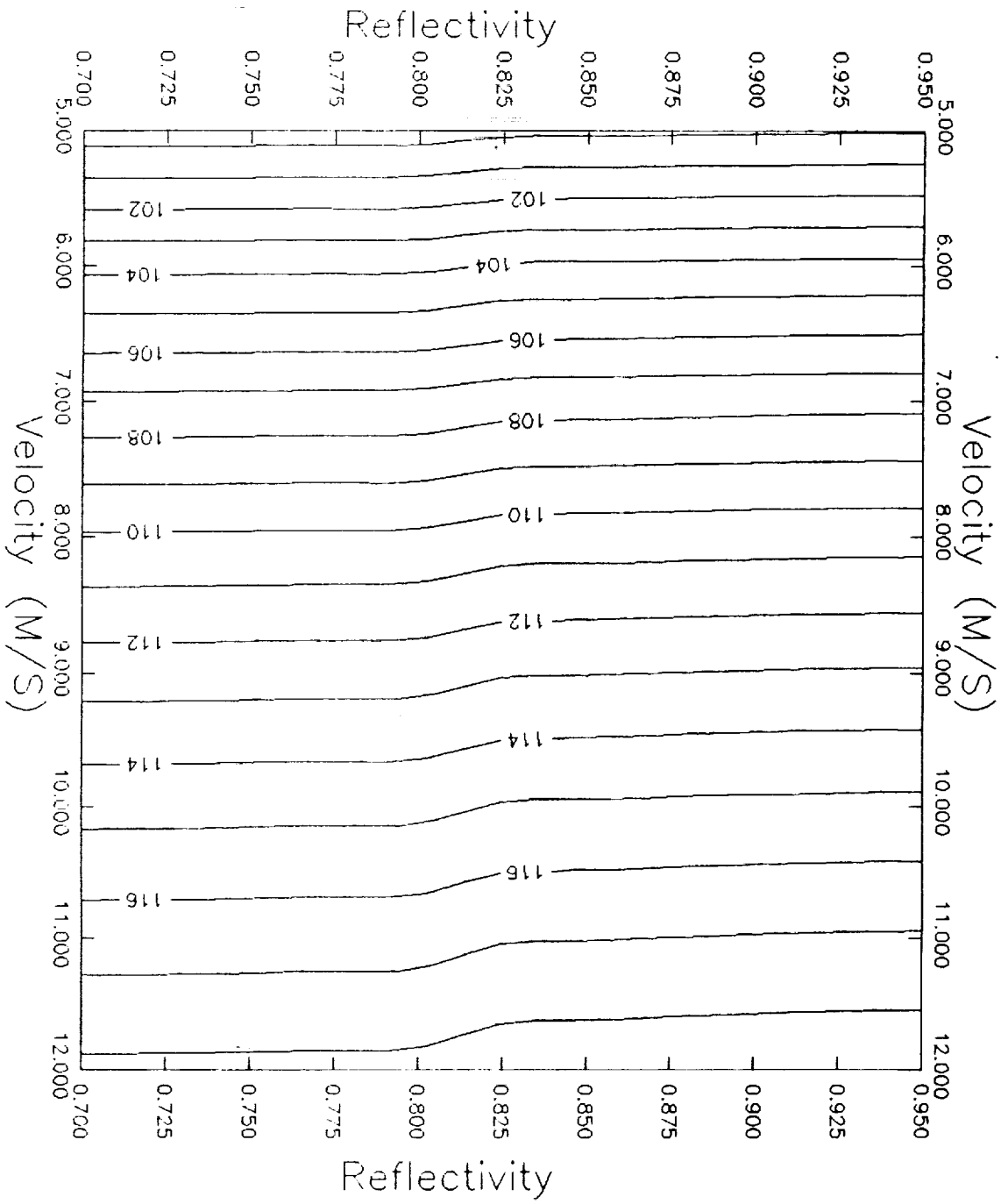

$L = 500\,\text{cm}$ $a = 15\,\text{cm}$ $frac = 0.0005$

Figure A4(b) Simulated $t - C_4F_9$ Space Laser

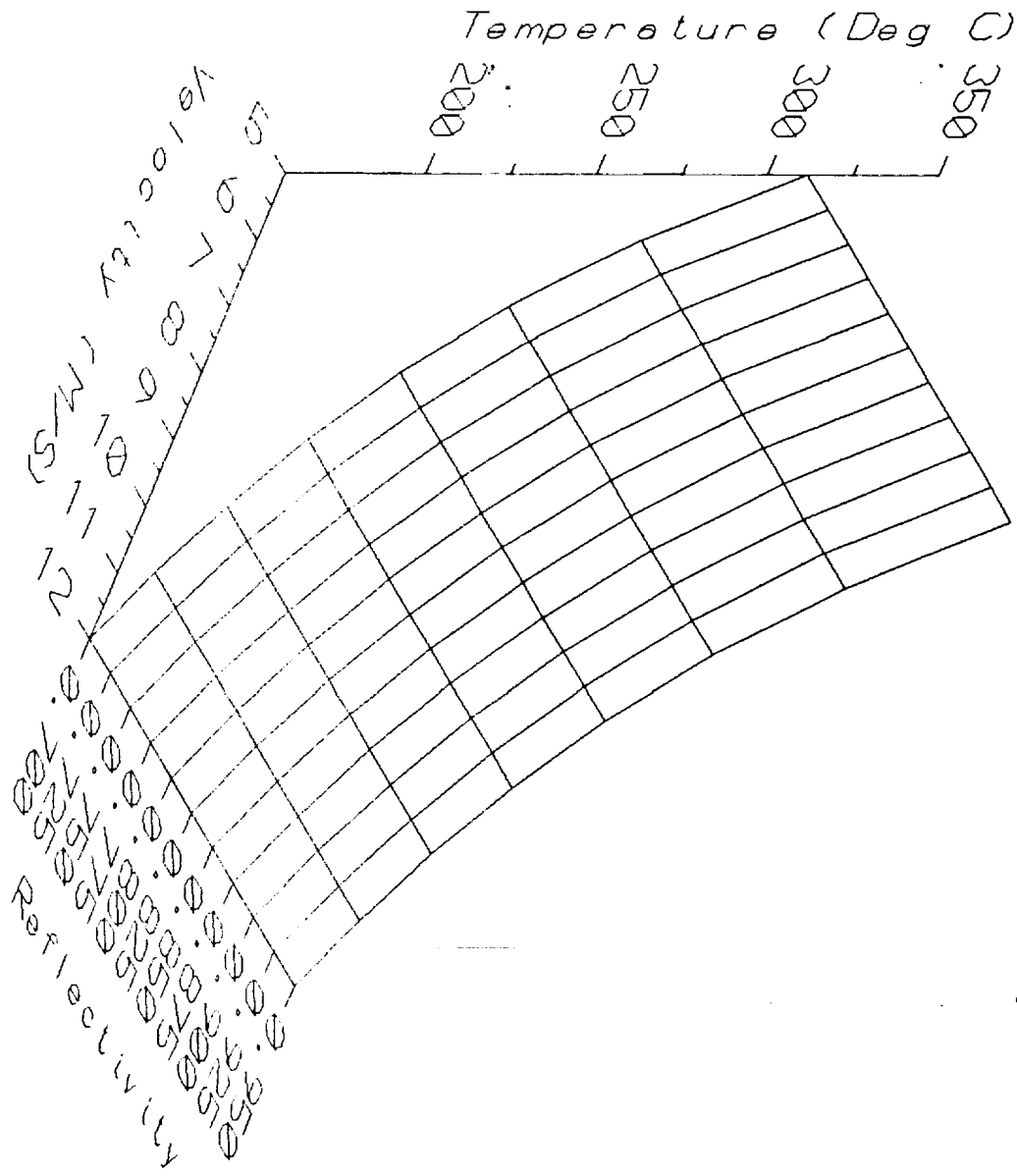

Figure A4(c) Simulated $t - C_4F_9$ Space Laser

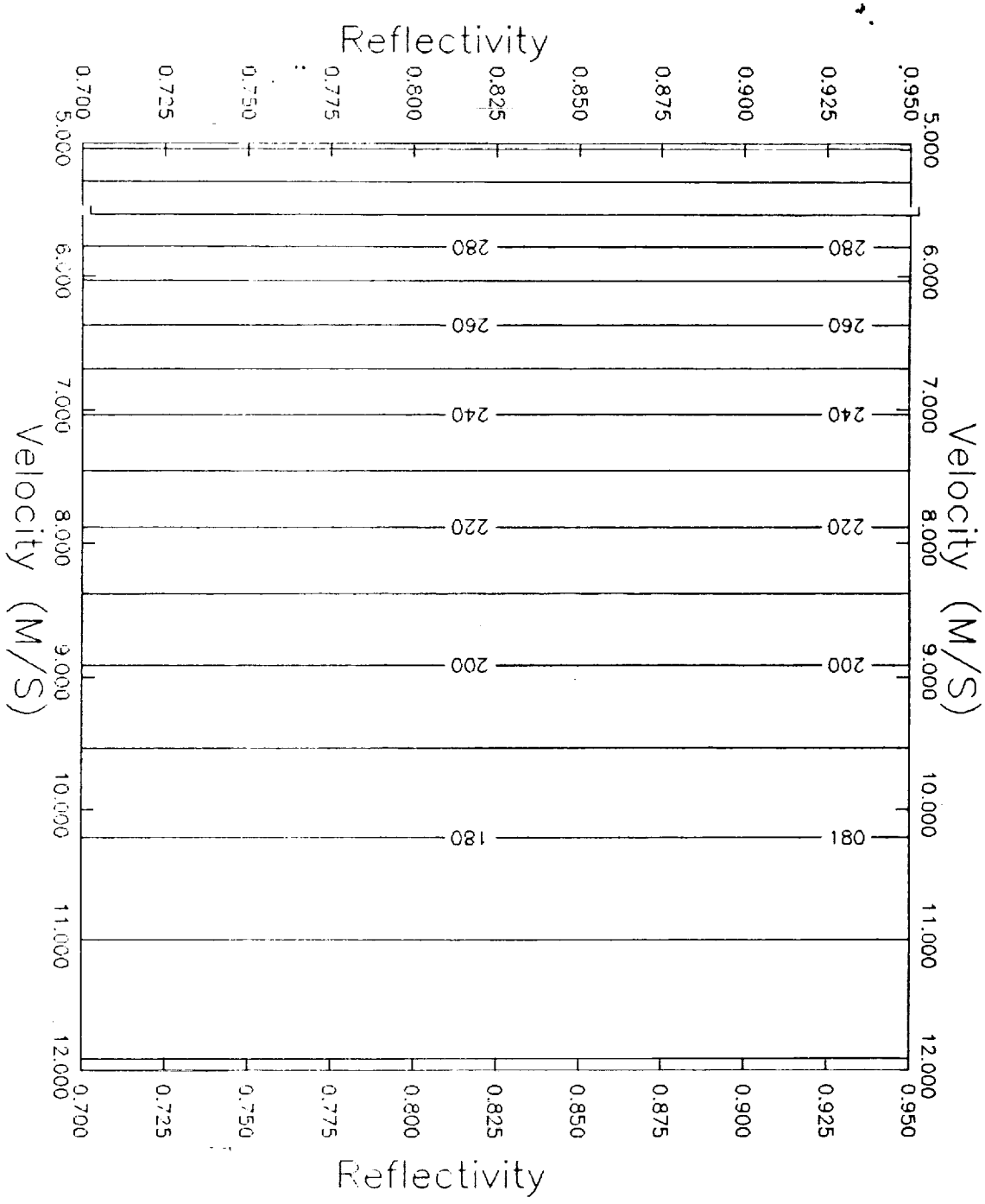

$L = 500\,\text{cm}$ $a = 15\,\text{cm}$ $frac = 0.0005$

Figure A4(d) Simulated $t - C_4F_9$ Space Laser

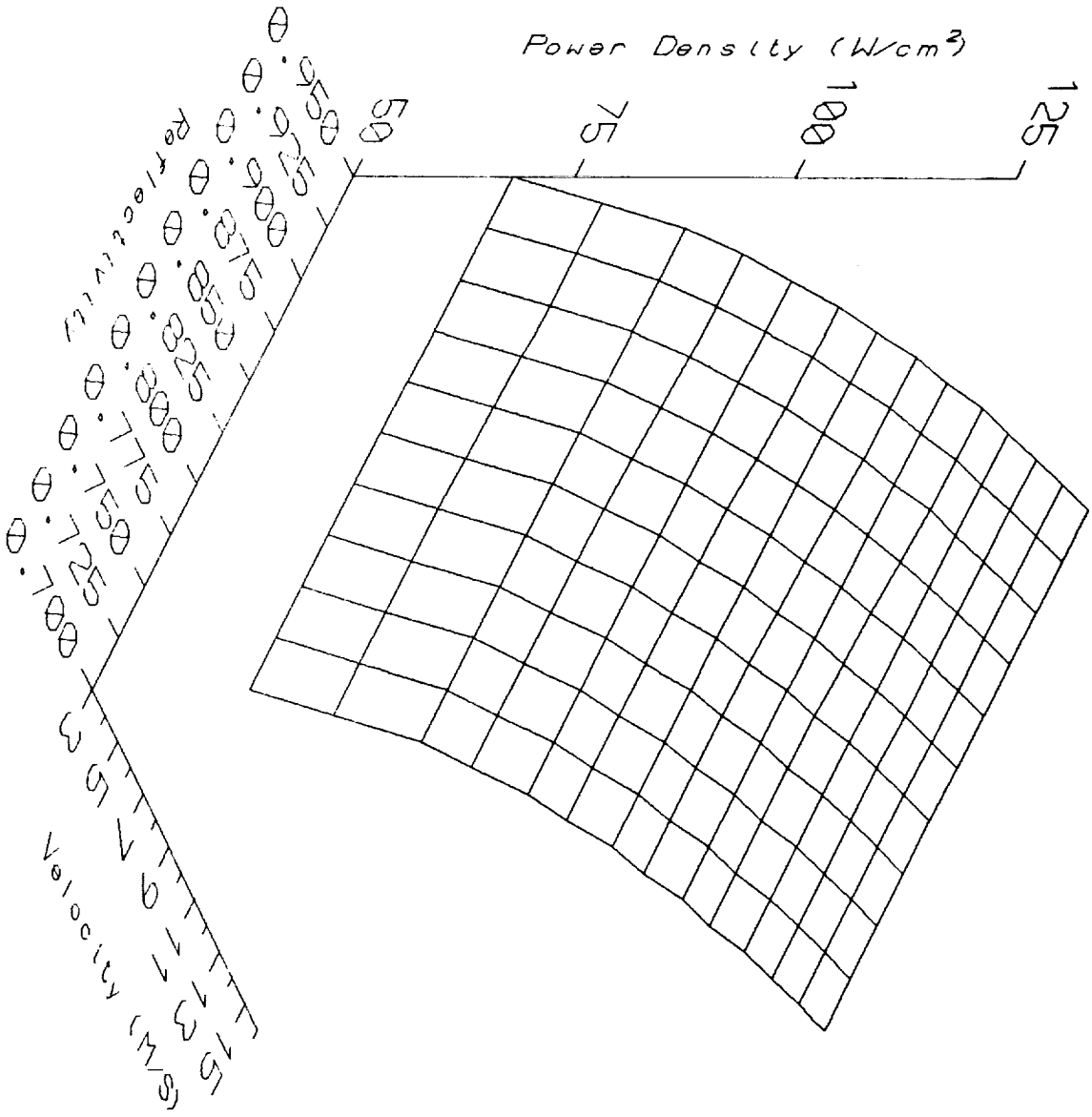

t-C4F9I with Troc=.001

Figure A5(a) Simulated $t - C_4F_9I$ Space Laser

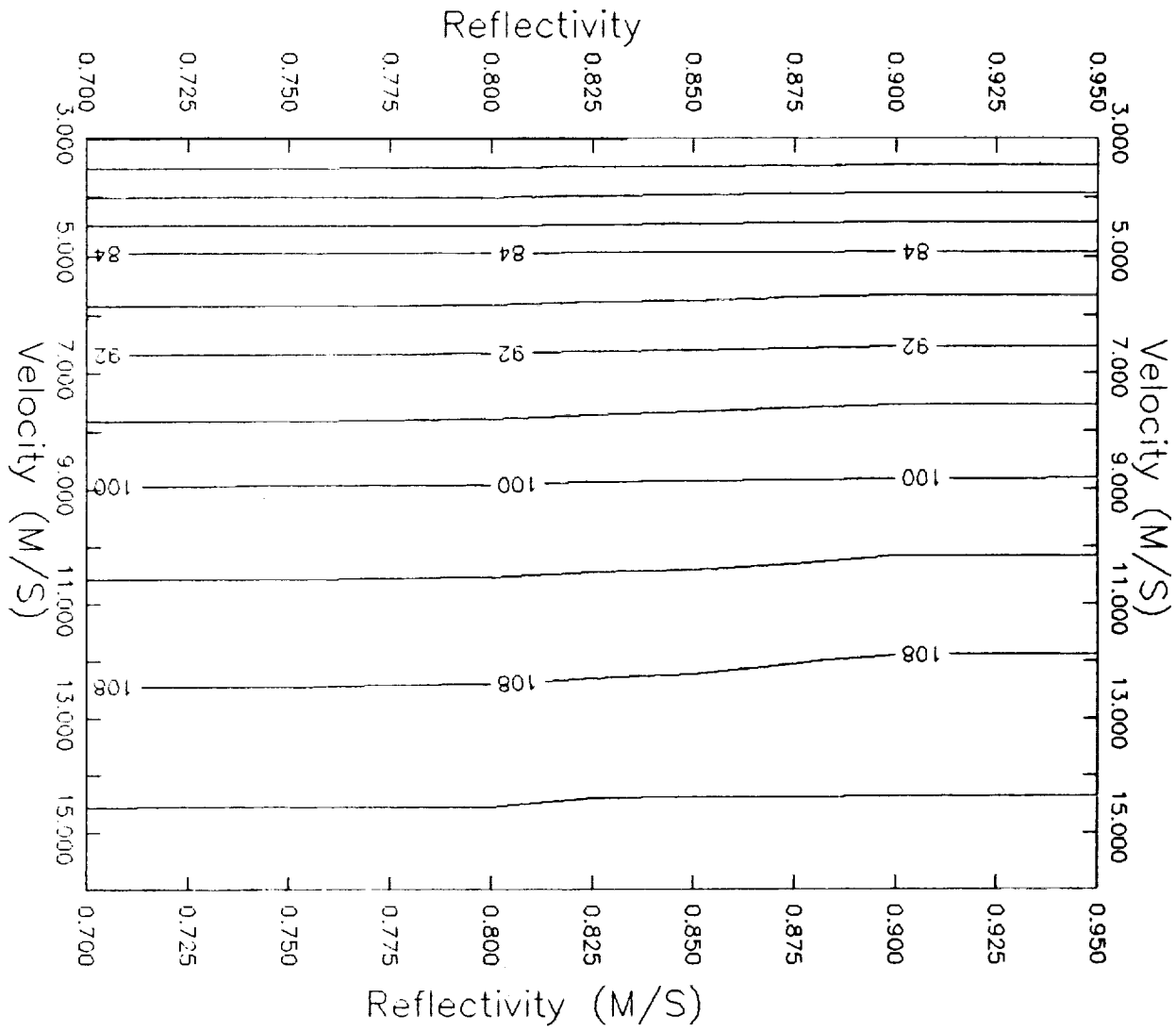

Figure A5(b) Simulated $t - C_4F_9I$ Space Laser

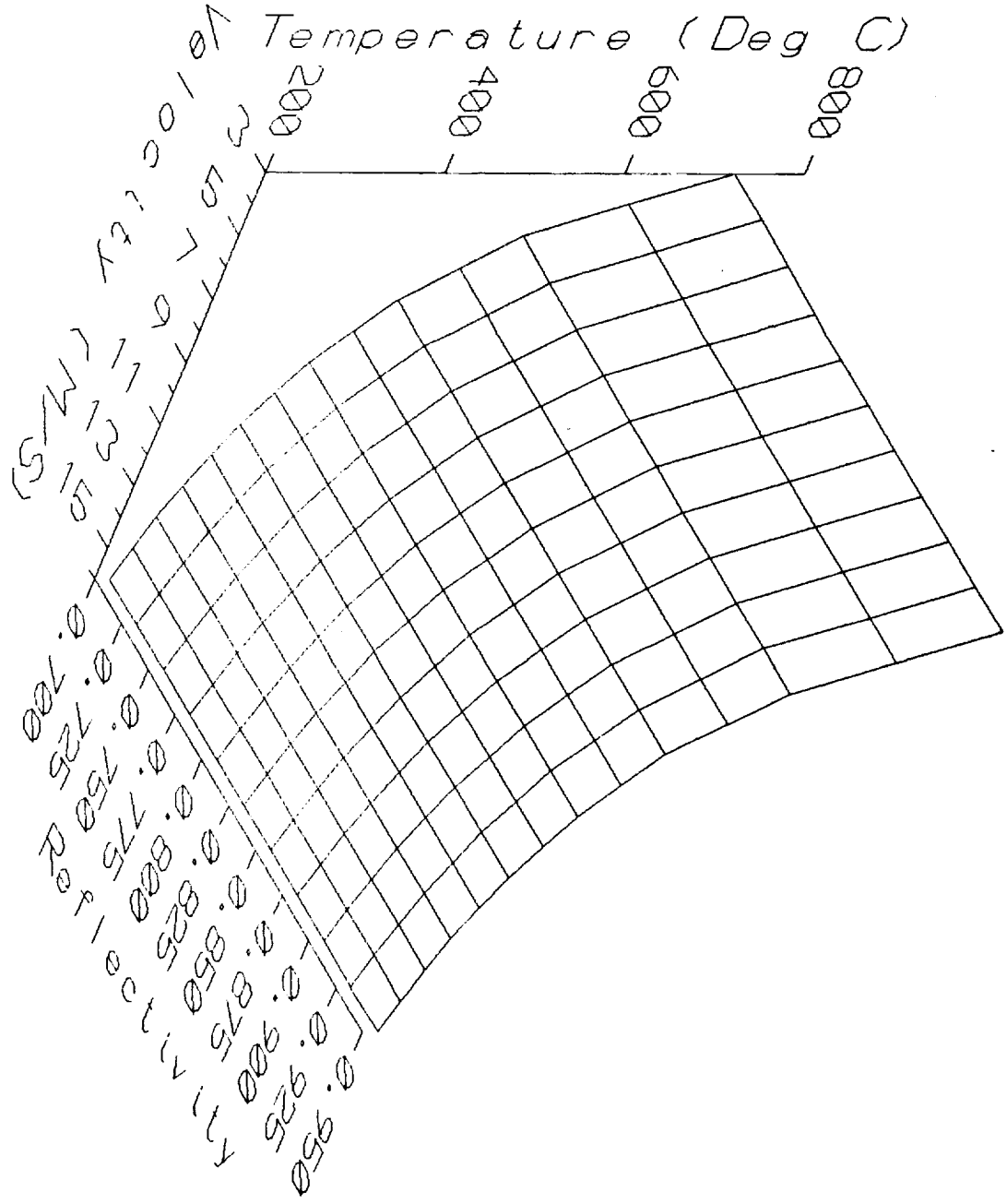

t-C_4F_9I with frac=.001

Figure A5(c) Simulated $t - C_4F_9I$ Space Laser

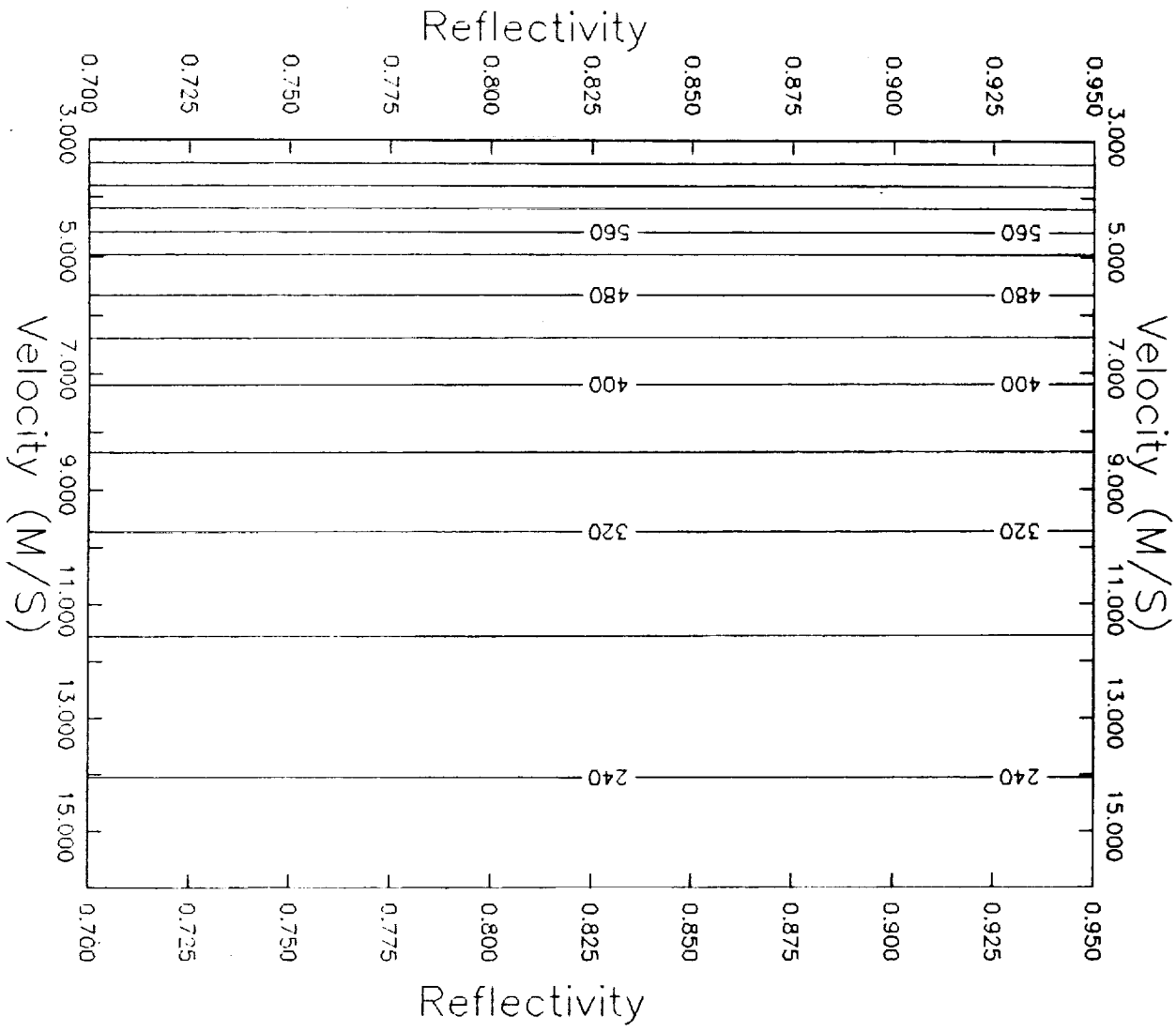

Figure A5(d) Simulated $t - C_4F_9I$ Space Laser

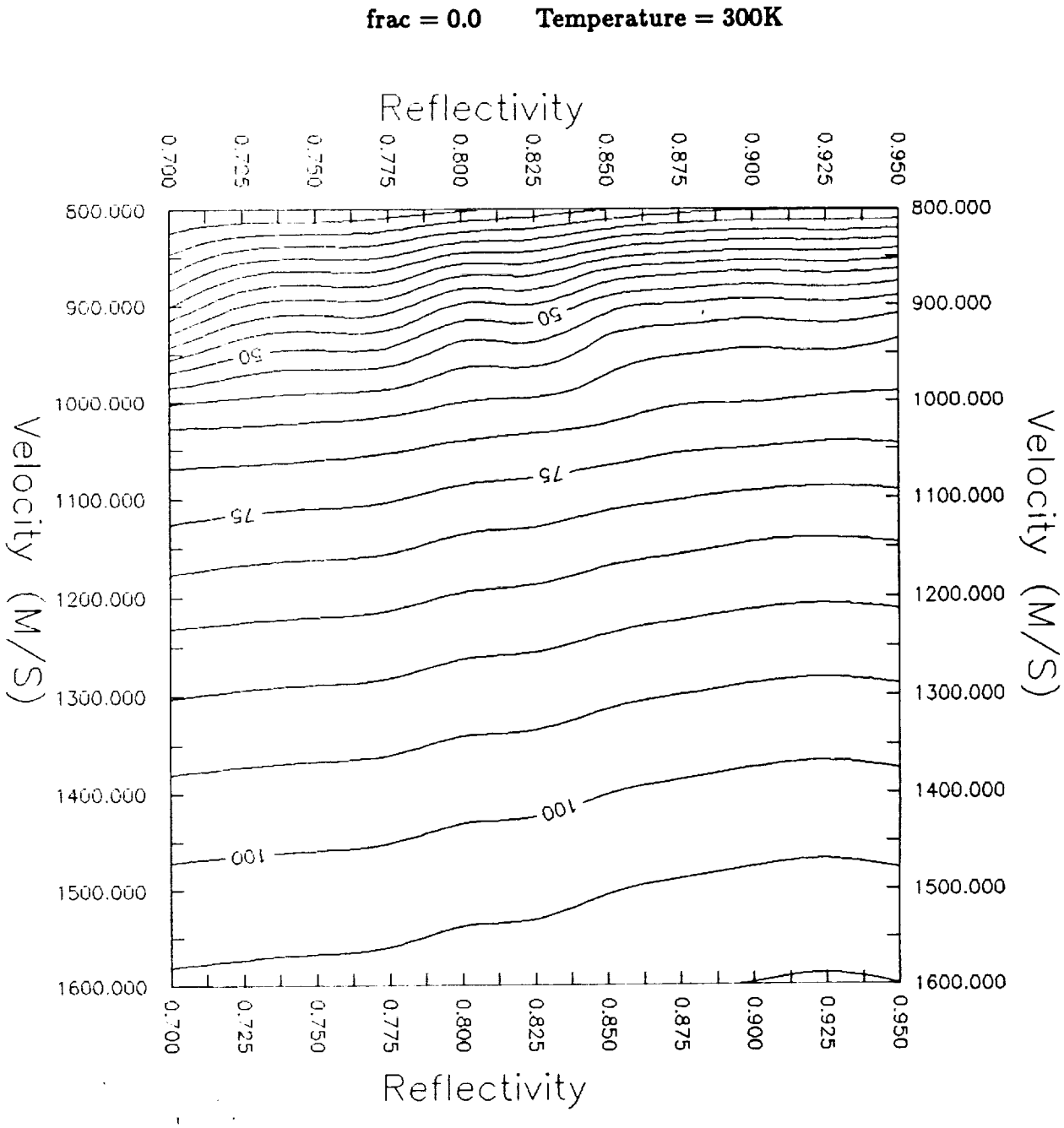

Figure A6(a) Simulated $t - C_4F_9I$ Space Laser

frac = 0.0 Temperature = 300K

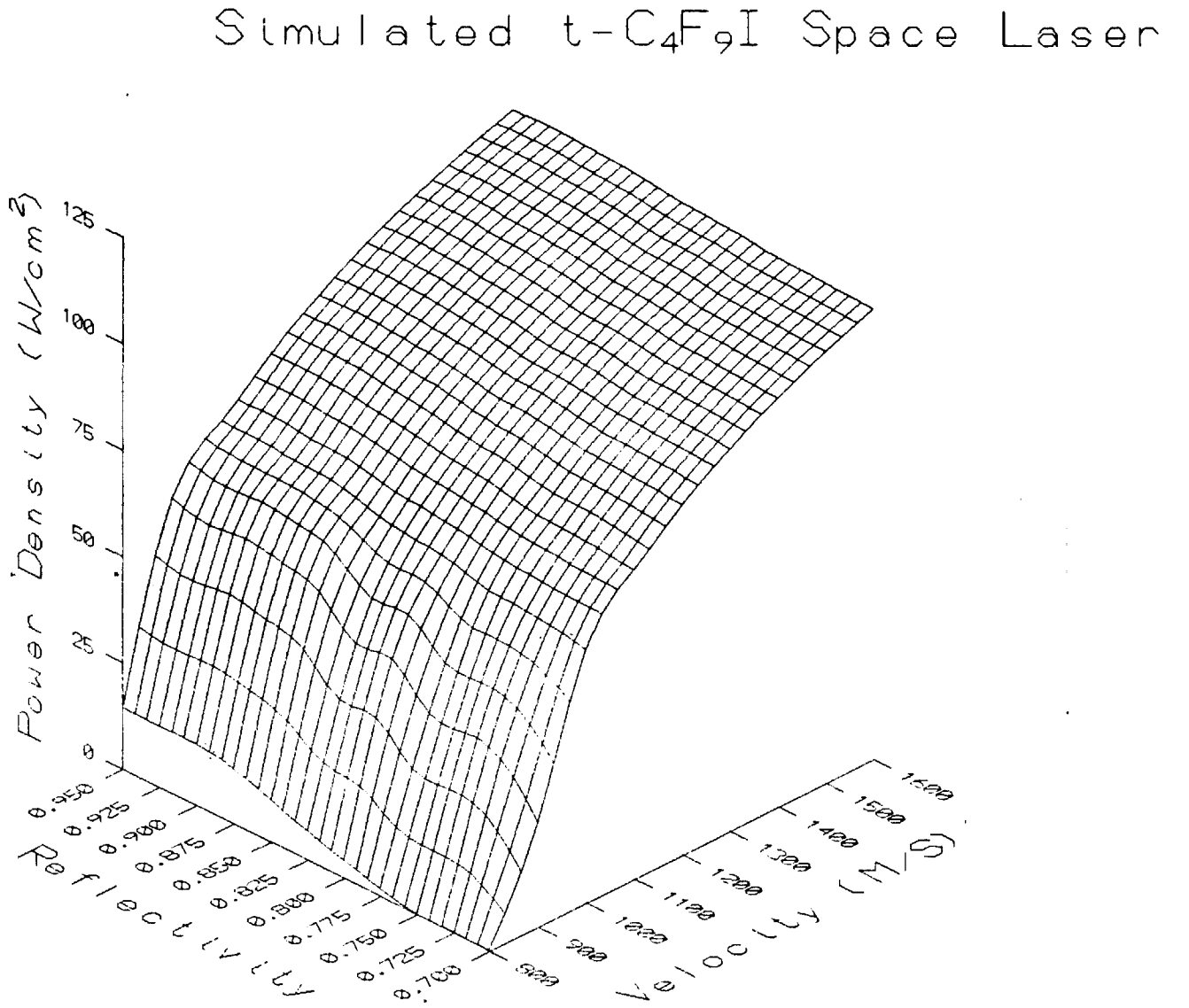

Figure A6(b) Simulated $t - C_4F_9I$ Space Laser